frontiers | Frontiers in Materials

TYPE Mini Review
PUBLISHED 18 March 2025
DOI 10.3389/fmats.2025.1561198

OPEN ACCESS

EDITED BY
Junqi Wang,
Xi'an Jiaotong University, China

REVIEWED BY
Youbin Zheng,
University of Liverpool, United Kingdom
Bolang Cheng,
Xiangtan University, China
Jie Qiu,
Shanghai Jiao Tong University, China

*CORRESPONDENCE
Duoqiang Pan,
panduoqiang@lzu.edu.cn
Weiwei Wu,
wwwu@xidian.edu.cn

RECEIVED 16 January 2025
ACCEPTED 03 March 2025
PUBLISHED 18 March 2025

CITATION
Chen J, Zhang X, Xiao W, Pan D and Wu W (2025) Advances in gadolinium-based composite materials for neutron and gamma-ray shielding.
Front. Mater. 12:1561198.
doi: 10.3389/fmats.2025.1561198

Advances in gadolinium-based composite materials for neutron and gamma-ray shielding

Jian Chen[1,2], Xingwu Zhang[1], Weixiang Xiao[1], Duoqiang Pan[2]* and Weiwei Wu[3]*

[1]Yangjiang Nuclear Power Co. Ltd., Yangjiang, Guangdong, China, [2]Radiochemistry and Nuclear Environment Laboratory, School of Nuclear Science and Technology, Lanzhou University, Lanzhou, China, [3]Interdisciplinary Research Center of Smart Sensors, Shaanxi Key Laboratory of High-Orbits-Electron Materials and Protection Technology for Aerospace, School of Advanced Materials and Nanotechnology, Xidian University, Xi'an, Shaanxi, China

With the significant advancements in nuclear technology, countries have invested considerable research into radiation shielding and protection materials. Neutrons and gamma photons have strong penetrating abilities, which can directly jeopardize human health or lead to the failure of electronic components. Therefore, developing high-performance materials for neutron and gamma photon radiation shielding has become a critical priority. Gadolinium (Gd), a rare earth element with the largest neutron absorption cross-section among natural elements, performs excellently as a neutron absorber. Gd-containing radiation composite shielding materials are typically classified into four main categories based on their matrix: metal-based, glass-based, ceramic-based, and polymer-based. This paper reviews the current research status of these four types of radiation shielding materials. It provides a comprehensive summary and evaluation of each material's preparation processes, microstructures, mechanical properties, and shielding performance. Additionally, the paper discusses the role of Gd in each type of matrix material and addresses the current challenges in the field.

KEYWORDS

radiation shielding, neutron, gamma, gadolinium, composite materials

1 Introduction

Nuclear technology, with its significant advantages, is now widely implemented across various sectors, including industry, healthcare, environmental conservation, and agriculture. Its applications range from clean nuclear energy production and neutron capture for cancer therapy to neutron irradiation for material modification and radiation detection (Hu et al., 2020; Rehm, 2022; Shruti and Gurmeet, 2022; Rehm, 2023). However, despite the benefits of nuclear energy, it also poses risks, including damage to electronic components and threats to human life and health. The primary concern stems from the formidable penetrating power of neutrons and gamma rays, which can easily pass through clothing and the outer layers of human skin, causing severe damage to cells, tissues, and even genetic material (Glass, 1957). Studies show that high levels of gamma radiation raise the risk of cancer and leukemia (Do et al., 2019; Boice et al., 2022). Additionally, prolonged radiation exposure can cause irreparable damage to electronic equipment and instruments. Therefore, the development of effective radiation

shielding materials to mitigate the hazards of nuclear radiation has become a crucial and urgent task.

In 1954, the Soviet Union established the world's first commercial nuclear power plant at the Institute of Physics and Power Engineering (IPPE) in Obninsk, catalyzing the development of large-scale nuclear power and technology (Rachkov et al., 2014). As nuclear technology continues to expand, traditional shielding materials are increasingly inadequate for the growing range of applications. For example, lead, one of the earliest protective materials, has high density, good ductility, and effective attenuation of X-rays and gamma rays (Jayakumar et al., 2023). However, its toxicity limits its use. Concrete, commonly used as structural shielding material, is cost-effective and has a larger mass but lacks mobility, making it suitable only for large-scale load-bearing equipment (Onaizi et al., 2024). Boron has a relatively large neutron absorption cross-section, with good neutron absorption, but its high brittleness is expensive and unfavorable for processing. Other protective materials, such as water, graphite, iron, etc., only in a single radiation scenario with a certain degree of protection, can only be in environmentally restricted conditions to play a specific role. As a result, research is focused on developing lightweight, high-strength radiation protection materials. Consequently, significant financial and scientific resources have been allocated to this area.

Rare earth elements (REEs) constitute a series of 17 metal element families (La-Lu) consisting of group III (Sc, Y) and lanthanides (Hu et al., 2006; Schelter, 2019). Rare earth elements possess distinctive 4f valence electron orbitals. The combination of domain fixation and incomplete filling of the 4f electrons, coupled with their high valence, large radius, and strong polarization force, makes rare earth elements an invaluable resource in the preparation of magnetic materials, luminescent materials, catalysts, radiation shielding, and other applications (Anishur Rahman et al., 2010; Al-Buriahi et al., 2019; Schelter, 2019; Alharshan et al., 2022; An et al., 2023; Peng et al., 2023). Among the entire range of rare earth materials, gadolinium (Gd) is distinguished by the fact that its outer electrons are only partially filled, making it the atom with the greatest number of unpaired electrons in the entire group. Its electronic configuration ($4f^7 5d^1 6s^2$) contributes to an enlarged atomic radius and facilitates the formation of vacancy defects in its crystalline lattice (Dorenbos, 2013). These structural characteristics enhance inelastic scattering interactions with neutrons, which serve to moderate neutron energy and increase the probability of subsequent neutron-nucleus interactions. Furthermore, Gd demonstrates the highest neutron absorption cross-section within the rare earth family (Wang et al., 2023). Natural Gd is typically found in the form of Gd_2O_3. A number of its nuclides, including ^{157}Gd, exhibit the largest neutron absorption cross-section of 255,000 b, while ^{155}Gd displays a thermal neutron absorption cross-section of 62,540 barns, outperforming conventional boron-based absorbers by several orders of magnitude (other isotopes such as ^{158}Gd contribute relatively little to neutron capture) (Hidaka et al., 2000). Furthermore, its n and γ reaction cross-sections for thermal neutrons are observed to be tens of times higher than those observed for boron. The total content is as high as 30 wt% (Kregl et al., 2017; Wang et al., 2022). With an atomic number (Z = 64) second only to high-Z elements such as lead, Gd achieves superior gamma-ray attenuation through multiple mechanisms, including photoelectric absorption and Compton scattering.

Compared to hydrogen-rich materials, Gd-based systems uniquely enable simultaneous attenuation of both primary neutrons and secondary gamma rays generated during neutron capture events. When contrasted with boron-containing materials, Gd offers enhanced shielding efficiency across broader energy spectra while circumventing performance degradation caused by hydration issues inherent to boric acid-based compounds. Therefore, Gd represents one of the most significant components employed as a shielding and fluxing device in the field of nuclear power (Yousefi et al., 2015), exhibiting exceptional neutron absorption capabilities.

With the rapid advancement of nuclear technology, there has been an increasing interest in the research and development of shielding and protection materials. However, the research progress with Gd as a shielding material has been relatively underdeveloped. This paper aims to highlight the advantages of Gd as an effective neutron shielding material. It will examine the interaction mechanisms between neutrons, gamma rays, and Gd, and review the current state of research on Gd in various substrate materials. Finally, we evaluate the prospective applications of Gd-based neutron shielding materials in the context of existing challenges, including dynamic radiation environments and multifunctional performance requirements.

1.1 Neutron interactions with the rare earth element Gd

Neutrons are generally electrically neutral, and their interaction with electrons in matter is minimal. It can be observed that the energy loss of these particles is not primarily due to ionization and excitation of atoms. Instead, their energy is lost predominantly through collisions with atomic nuclei (Soltan, 1938). Neutrons can be classified into three principal categories according to their energies: fast neutrons (E > 0.1 MeV), medium-energy neutrons (1 keV < E < 100 keV), and slow neutrons (E < 1 keV). Additionally, neutrons with an energy of 0.0253 eV are commonly designated as "thermal neutrons."

Neutron interactions with matter can generally be categorized into two types: scattering and absorption. The former encompasses both elastic and inelastic scattering. The lowest excitation energy level of medium and heavy nuclei is low, and their first excitation energy level is generally around 0.1~1 MeV. Fast neutrons have a higher energy level than the lowest excitation energy level of the target nucleus. Accordingly, high-energy fast neutrons will initially undergo inelastic collisions with medium and heavy nuclei, thereby decreasing their kinetic energy following the interaction with target nuclei and reducing them to fast neutrons. Afterward, following the law of conservation of kinetic energy, fast neutrons will undergo elastic collisions with light nuclear elements, resulting in a rapid reduction in neutron energy. Ultimately, these neutrons will have a high neutron capture cross-section in the material capture reaction, which can be absorbed by γ light. This process can also be observed in heavy nuclear elements.

As shown in Table 1, the thermal neutron absorption cross-sections for several common elements are illustrated, with Gd being the rare earth element possessing the largest neutron absorption cross-section. For neutrons, Gd with natural isotopic abundance (containing 15.7% ^{157}Gd and 14.8% ^{155}Gd) exhibits

TABLE 1 Thermal neutron absorption cross-sections of several elements.

Element	A	Neutron capture cross-section (barn)	Abundance (wt%)
B	10	3,837	19.9
Gd	155	62,540	14.8
	156	1.71	20.4
	157	255,000	15.65
Sm	149	40,000	13.8
Eu	153	4,500	52.2

an exceptionally high macroscopic absorption cross-section ($\Sigma_a \approx 1.42\ cm^{-1}$) at thermal neutron energies (0.025 eV) (Ho et al., 2022). Furthermore, its key isotopes, ^{155}Gd and ^{157}Gd, demonstrate strong resonance absorption in the epithermal neutron range (G. Leinweber et al., 2006). However, the neutron absorption efficiency of Gd significantly declines for fast neutrons (>1 MeV, $\Sigma_a < 0.5\ cm^{-1}$), necessitating the use of moderating materials (e.g., polyethylene, water) to enhance shielding performance (Li X. et al., 2024). Gd can combine with light elements, utilizing elastic and inelastic scattering to slow down high-energy neutrons. Ultimately, it absorbs lower-energy neutrons and the resulting secondary gamma photons, achieving optimal shielding.

1.2 Interaction of gamma photons with the rare earth element Gd

Gamma rays (γ-rays) were first discovered by the French scientist Villars in 1900 (Gerward, 1999). γ-rays are high-energy photons that are massless and uncharged, which allows them to easily penetrate materials. They can be generated naturally through the radioactive decay of radionuclides (e.g., 238U and 232Th series) or artificially in nuclear reactors (Eman et al., 2021). γ-rays interact with matter primarily through three mechanisms: photoelectric effect, Compton scattering effect, and electron pair effect.

The photoelectric effect occurs when an incident photon interacts with an atom, transferring all its energy to an electron. This energy causes the electron to overcome the binding forces of the atom and be ejected from the atom. The ejected electron is called a photoelectron, and the photon ceases to exist. As the atom returns to its ground state through de-excitation, it may emit an Auger electron or an X-ray, as shown in Figure 1a. The likelihood of the photoelectric effect occurring is quantified by the photoelectric cross-section (σph), which is positively correlated with the fifth power of the atomic number (Z) and negatively correlated with the photon energy (hυ). Therefore, high-Z materials are more efficient at absorbing low-energy photons through this mechanism.

As shown in Figure 1b, Compton scattering involves an inelastic collision between an incident photon and an outer electron, resulting in the transfer of some energy to the electron, which causes it to be ejected from the atom as a recoil electron. The photon, now with reduced energy, is scattered at a different angle. Compton scattering is the dominant mechanism through which matter interacts with neutral energy. Similar to the photoelectric effect, the probability of Compton scattering is described by the Compton scattering cross-section (σC), which is proportional to the atomic number (Z).

The electron pair effect, as illustrated in Figure 1c, occurs when an incident photon passes near the nucleus of an atom and is converted into a positron and an electron due to the Coulomb field of the nucleus. The positron and electron subsequently interact with nearby atoms, losing energy and slowing down due to Coulomb forces. Eventually, the positron annihilates with an electron in the material, producing two gamma photons, each with an energy of 0.511 MeV. The electron pair cross-section (σp) is proportional to the square of the atomic number (Z^2). High-energy photons interacting with elements or compounds of high atomic number are more likely to result in pair production, leading to enhanced radiative attenuation (Zhang Q.-P. et al., 2020). Figure 2 illustrates the correlation between these three effects, photon energy, and atomic number. It is evident that elements with higher atomic numbers demonstrate superior γ-ray shielding capabilities.

There are various mechanisms by which photons interact with matter, mainly dominated by the photoelectric effect, the Compton scattering effect, and the electron pair effect (Kaur et al., 2016). σ_t denotes the cross-section of the ray-matter interaction, then

$$\sigma_t = \sigma_{ph} + \sigma_c + \sigma_p$$

Figure 2 represents the relationship between the three effects and the atomic number of the photon energy. When the material has a large atomic number, the photoelectric effect dominates when the incident photon energy is low, and the electron pair effect dominates when the incident electron energy is high. When the atomic number of the material is low, Compton scattering dominates.

2 Research progress of Gd-based composite shielding materials

In recent years, rare earth elements have exhibited good radiation protection properties and have become a research hotspot in radiation composite shielding materials. Gd-based composite shielding materials can be classified by substrate (Figure 3). metal-based composite shielding materials, glass-based composite

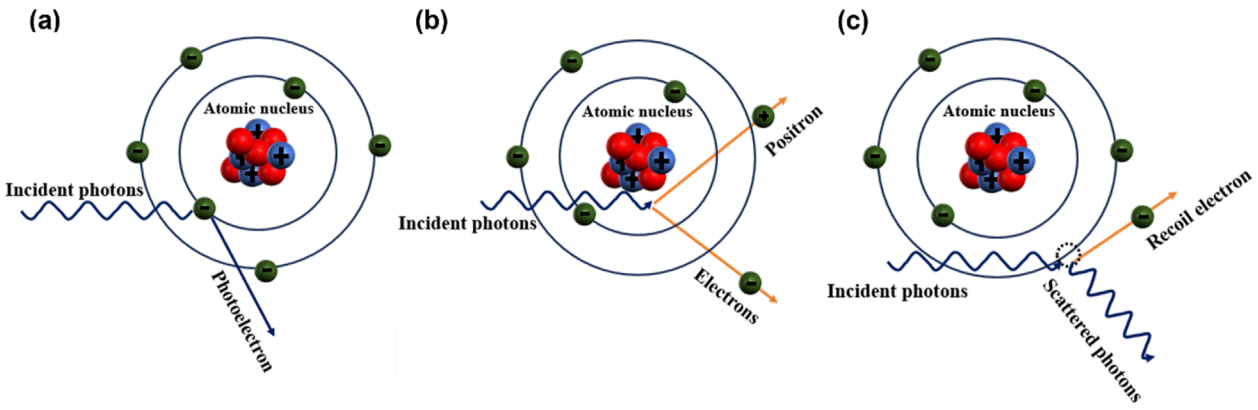

FIGURE 1
Three types of interactions between Gamma rays and matter: **(a)** Photoelectric effect, **(b)** Compton scattering, and **(c)** Electron pair effect.

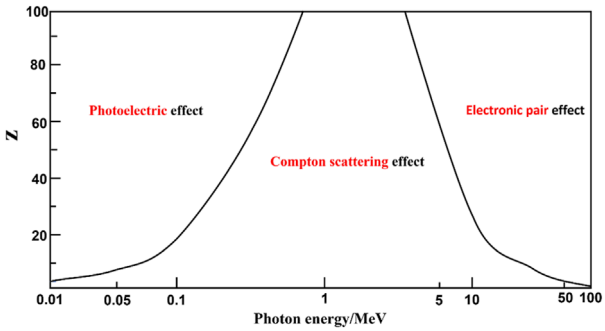

FIGURE 2
The relationship between the three interaction mechanisms, photon energy, and atomic number.

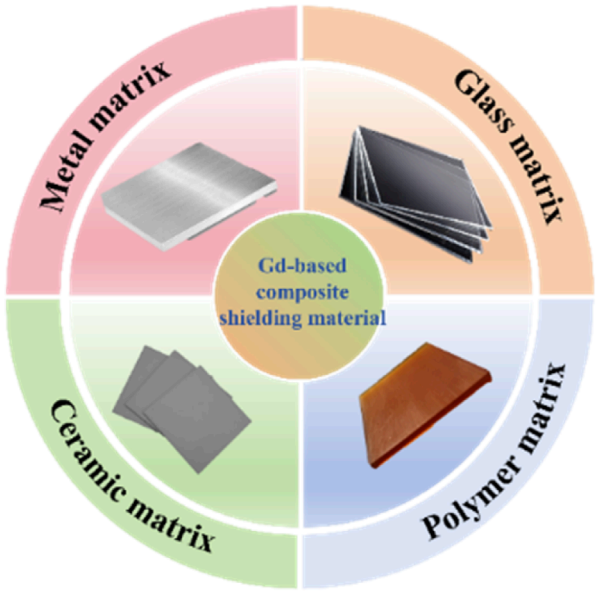

FIGURE 3
Classification of Gd-containing composite radiation shielding materials.

shielding materials, ceramic-based composite shielding materials, and polymer-based composite shielding materials.

2.1 Gd-containing metal matrix composite shielding materials

For stationary power reactors such as nuclear power plants, shielding materials must balance three key parameters: shielding performance, total weight, and volume, to comply with design specifications. Cost-effectiveness is also a crucial consideration. Metal-based composite shielding materials offer superior mechanical properties, corrosion resistance, and workability, though their higher production costs can be advantageous in space-constrained nuclear installations. However, their cost-effectiveness remains relatively low, which presents challenges in certain nuclear facilities with limited space (Gupta, 2020; Gan et al., 2021). Currently, metal-based composite shielding materials can be classified into iron-based, aluminum-based, stainless steel-based, and other metal-based composites. Among these, Gd-containing metal-based composites are primarily aluminum-based and stainless steel-based, as shown in Table 2.

Aluminum, due to its low density, ease of processing, and relatively low cost, is an excellent choice as a matrix material for mass-produced metal-based shielding. The high thermal neutron absorption cross-section of ^{10}B enables the effective absorption of thermal neutrons via the ^{10}B (n, α) ^{7}Li transmutation reaction (Zhang et al., 2008; Xu et al., 2016a). Moreover, the use of ^{10}B as a reinforcing filler, such as in boron steel or boron carbide (B_4C)/Al metal composites, has been widely applied for the storage and transportation of spent nuclear fuel. However, the shielding capacity of boron steel for thermal neutrons is negligible when the concentration of ^{10}B is low, and excessive concentration can lead to a deterioration in the mechanical properties of the composites. Increasing the content of boron carbide (B_4C) raises

TABLE 2 Some Gd-containing metal matrix composite shielding materials and their performance parameters.

Year	Composition	Mechanical properties	Shielding performance	References
2016	(15%B_4C+1%Gd)/Al	Elongation 9%	Neutron capture rate~99% (Thickness 3 mm), Transmission cross-section Σ = 21.3 cm^{-1}	Xu et al. (2016b)
2024	15% Gd_2O_3/Al	—	Thermal neutron macroscopic cross-section Σ = 71.0 cm^{-1}	Kursun et al. (2024)
2019	10wt% Gd_2O_3/6061Al	Ultimate tensile strength 240 Mpa, Elongation 16%	Neutron capture rate 99.6261%	Zhang and Bai (2019)
2019	(15%B_4C+1%Gd)/6061Al	Tensile strength ~340 Mpa, Elongation ~9%	—	Xu et al., (2019)
2023	15wt.%SiC/5wt% Gd_2O_3/6061Al	Tensile strength 196 Mpa, Elongation percentage 11%	Neutron capture rate 99.8% (Thickness 1 mm)	Lian et al. (2023)
2022	TiB_2/Al-Mg-Gd	Tensile strength 464 ± 6 Mpa, Elongation 15.6% ± 0.4%	Neutron capture rate ~99% (Thickness 8 mm)	Chen et al., (2022)
2023	2wt.%Gd/Alloy (Austenitic 304, 316, and duplex stainless steel 5A)	304-Gd: Tensile strength 572.2 ± 67.3 Mpa, Elongation 38.3% ± 3.3% 316-Gd: Tensile strength 504.0 ± 15.6Mp, Elongation 49.4% ± 4.6% 5A-Gd: Tensile strength 776.5 ± 24.3 Mpa, Elongation 15.9% ± 5.1%	Neutron capture rate~99% (Thickness 0.5 mm)	Oh et al. (2023)
2024	4.8wt.%Gd/Boronized stainless steel	—	Neutron absorption cross-section Σ = 45.1 cm^{-1}	Ji et al. (2024)

the hardness of the material, which in turn limits its processability and moldability (Oh et al., 2023; Sun et al., 2023). Studies have shown that ^{157}Gd possesses a thermal neutron absorption capacity four times greater than that of ^{10}B, while also offering a cost advantage of approximately one-twelfth to one-fifth of that of ^{10}B (Xu et al., 2016b). Additionally, Gd can effectively reduce the formation of helium bubbles during the neutron absorption process, thereby extending the lifetime of neutron-absorbing and shielding materials (Cong et al., 2020; Jung et al., 2020). Thus, replacing B with Gd offers a solution to the content-performance dilemma.

Through the strategic partial substitution of Gd for B_4C in B_4C/Al composites, Xu et al. (2016a) successfully alleviated the constraints induced by tensile brittleness, which hindered the development of shielding composites. This modification resulted in an improvement in the plasticity of the composites. As shown in Figure 4, the (15%B_4C + 1%Gd)/Al composites prepared by hot-pressing were compared with the conventional 30%B_4C/Al composites. The (15%B_4C + 1%Gd)/Al composite exhibited slightly better neutron shielding performance than the 30%B_4C/Al composite, with the elongation at break increasing from 4% to 9%. This research highlights an optimal combination of high neutron absorption and good ductility, making it a promising candidate for future neutron shielding applications. Kursun et al. (2024) employed a powder processing mechanical milling method to synthesize metal nanocomposites. Mechanical ball milling resulted in reduced grain size and refinement, facilitating the uniform fusion of aluminum, Gd, and oxygen elements. Similarly, it was found that lower concentrations of Gd_2O_3 were sufficient to produce thermal neutron attenuation efficiencies comparable to those of standard Al/B_4C composites. To address a wider range of application scenarios for shielding materials and meet more diverse protection requirements, researchers have focused on developing non-homogeneous structures, including layered and shell-core structures. Gaylan and Avar (2024) investigated the structure, mechanical properties, and neutron shielding characteristics of Al-20%B_4C-x%Gd_2O_3 (x = 1, 3, 5) composites through high-energy ball milling. The MCNP6.2 simulation results indicated that the Al-20%B_4C-5%Gd_2O_3 composite exhibited the highest fast neutron absorption rate, while the Al-20%B_4C-5%Gd composite demonstrated the highest thermal neutron absorption rate. Zhang P. et al. (2020) prepared a Gd_2O_3@W/Al composite by coating a layer of tungsten on the surface of Gd_2O_3 particles. When Gd absorbs neutrons, it excites secondary gamma rays, which are blocked by the tungsten shell, achieving simultaneous shielding against neutrons and secondary gamma rays. This approach is particularly promising for applications such as spent fuel storage and transportation, or for mobile nuclear reactors.

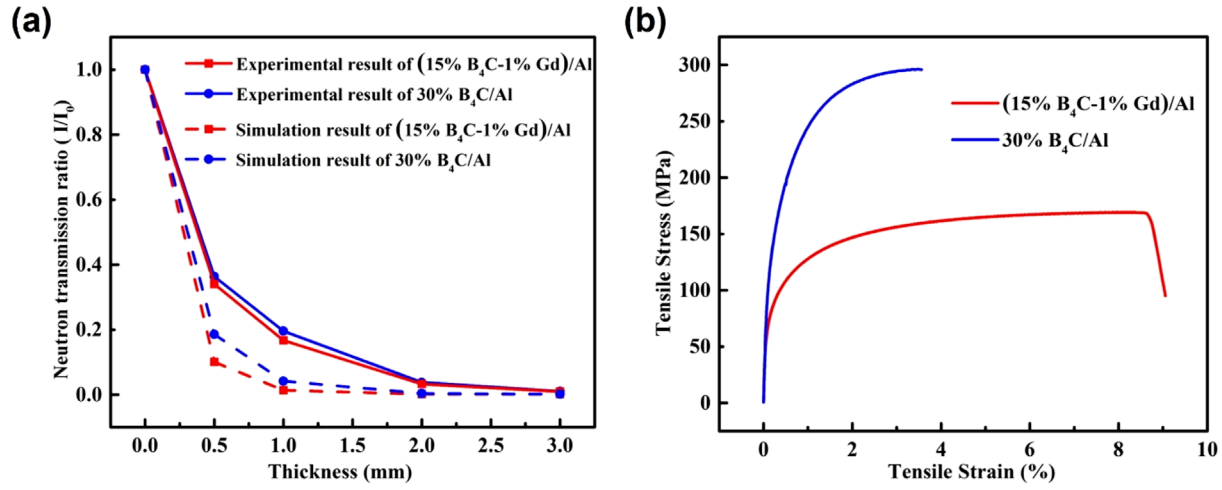

FIGURE 4
(15%B_4C-1%Gd)/Al and 30%B_4C/Al Composite Materials: **(a)** Neutron Transmission Rate and **(b)** Tensile Curve (Xu et al., 2016b).

Spent nuclear fuel (SNF) generated from nuclear reactors has an inherent spontaneous fission capability that releases intense neutrons and gamma rays, which are extremely hazardous to the environment and human beings and require careful and appropriate disposal (Wang et al., 2018; Fu et al., 2021; Qi et al., 2022). Boron-aluminum alloys have low melting points and mechanical strengths, making it difficult to meet the requirements of spent fuel storage racks and spent fuel transportation. Iron-based composite shielding materials are mainly based on stainless steel, which has excellent durability, corrosion resistance, and high strength. Combining it with boron can develop composite materials with neutron-shielding properties. However, boron has a very low solubility in stainless steel, making it extremely difficult to produce alloys with high shielding efficiency (Choi et al., 2013). Among the various types of stainless steels, duplex stainless steels with austenitic and ferrite phases have higher strength and better corrosion resistance than single-phase austenitic stainless steels at a lower cost (Yang et al., 2020; Qi et al., 2023; Silva et al., 2023). Choi et al. (2013) devised and manufactured a duplex stainless steel sheet with a Gd content of 1 wt% through a process involving melting, casting hot rolling, and solution treatment. The alloy consists of 31% ferrite phase and 69% austenite phase, and the main elements are chromium (Cr), nickel (Ni), and Gd. Gd-rich precipitates can be found inside the grains and at grain boundaries under microscopic conditions. Its ultimate tensile strength was 700.2 MPa, yield strength was 552.3 MPa, and elongation was 38.08%. Subsequently, this research team investigated the neutron-absorbing element Gd on the organization development characteristics and mechanical and corrosion behavior of duplex stainless steel in 2015 (Choi et al., 2016).

Oh et al. (2023) prepared alloys by adding 2 wt% of Gd to austenitic stainless steels 304 and 316 and duplex stainless steel 5A. The chemical composition of the alloys used in the experiments is presented in Table 3. It was determined that Gd was distributed uniformly in the alloy as an intermetallic compound, exhibiting no segregation or clustering. The mechanical properties were then compared with those of boronized stainless steel according to the ASTM A887 standard. The addition of Gd can increase the ultimate tensile and yield strength of the alloy by 11%. Despite a 48% reduction in elongation, the alloy exhibited significantly higher impact properties than boron-containing stainless steels. Kinetic potential polarization tests were carried out on the alloy, and the corrosion resistance of the alloy decreased with the addition of Gd, but its neutron absorption showed excellent performance. Baoting Ji et al. (2024) designed and prepared a new Gd-doped iron-based amorphous metal coating (Gd-AMC) using thermal spraying. The thermal neutron absorption cross-section of the coating containing 4.8 wt% Gd was observed to be 14.7 times higher than that of the borated stainless steel (BSS) substrate. Moreover, the authors propose a novel "dissolution passivation" process to rapidly form a protective passivation film on the amorphous substrate, resulting in localized corrosion resistance of the Gd-AMCs significantly better than that of the BSS substrate.

2.2 Gd-containing glass-based composite shielding materials

Glass is a distinctive material system, characterized by its inherent transparency (Kurtulus, 2024). This quality is particularly advantageous in contexts where optical clarity is paramount, such as control room windows, glass doors, protective panels for inspection systems, and radiation shielding sites, including those used for material testing and radiotherapy (Sayyed et al., 2019; Kawa and Kaky, 2024). Glass materials doped with rare-earth particles are extremely useful for the improvement of optical devices such as lasers, light propagators, optical fibers, amplifiers (Alalawi et al., 2022). Currently, glass systems used for radiation shielding are mainly classified as borates (Al-Buriahi et al., 2022), silicates (Albarzan et al., 2021), germinates (Sayyed et al., 2019), phosphates (Saudi et al., 2020), and tellurates (Kurtulus, 2024).

Borate-based glasses are the most extensively studied glass systems, known for their excellent metal oxide solvent properties.

TABLE 3 Chemical composition (wt%) of alloys used in the experiment (Oh et al., 2023).

Alloys	Fe	Cr	Ni	Mo	Mn	Si	N	Gd
304 (Amied)	Bal	18	10	—	1.3	0.8	0.1	2
304	Bal	18.4	9.21	—	1.01	0.45	0.13	—
304-Gd	Bal	18.1	9.44	—	1.13	0.62	0.12	1.76
316 (Amied)	Bal	18	12	2.4	1.3	0.8	0.1	2
316	Bal	19.3	11.6	1.9	1.4	0.91	0.12	—
316-Gd	Bal	18.3	10.9	2.12	1.19	0.77	0.14	2.13
5A (Amied)	Bal	25	7	4.5	1.3	0.8	0.3	2
5A	Bal	25.4	7.17	4.23	1.16	0.65	0.25	—
5A-Gd	Bal	25.8	7.63	4.34	1.22	0.78	0.28	1.96

This is due to the ability of their glass network to form tetrahedral units of BO_4 and triangular units of BO_3, which affords them the advantage of requiring a low processing temperature (Abou Hussein and Madbouly, 2024; Biradar et al., 2024). Yorulmaz et al. (2024) investigated the effect of different ratios of Gd_2O_3 on the structural, optical, radiation shielding, and mechanical properties of B_2O_3-Al_2O_3-Na_2O-Gd_2O_3 glasses. The radiation shielding parameters were determined at energies of 1,173 keV and 1,333 keV, respectively. The results demonstrated that the shielding was more effective at 1,173 keV than at 1,333 keV. Young's modulus of 104.211 GPa, fracture toughness of 1.215 MPa $m^{1/2}$, band gap energy of 2.89 eV, and LAC value of 0.1488 ± 0.0074 cm^{-1} were found to have optimum radiative and mechanical properties when the contribution of Gd_2O_3 was 3%. The disadvantage of B_2O_3 glass is the high phonon energy, which can be reduced by increasing the density of the glass. The density can be increased by adding heavy WO_2 and Gd_2O_3 components to the glass network. In 2021, Kaewnuam et al. (2022) prepared WO_3-Gd_2O_3-B_2O_3 glass by melt quenching. The high-density material has tremendous photon interaction and high radiation resistance, and the WGB glass increases with the concentration of Gd_2O_3. As shown in Figure 5, WGB glass appears a pale-yellow color that can be seen by humans and can be used as a radiation-shielding window. At 662 keV photon energy, the HVL of WGB glass is compared with that of commercial window glass and some standard shielding materials, and the HVL of the prepared WGB glass is in the range of 1.331 ~ 1.412 cm, and its Radiation shielding performance is superior to that of standard materials, among which the Gd17.5 glass has the best radiation shielding performance, and it is a promising shielding material of γ-rays at room temperature and high temperature. It is a promising shielding material for room temperature and high-temperature γ-rays. Alamosa et al. (Almousa et al., 2024) explored the role of mixtures of silicon (Si) and Gd rare earths in oxide glass matrices, which led to a new field of B_2O_3-SiO_2-Gd_2O_3 glass composites. The radiation shielding parameters were evaluated using the MCNPX code and the Phy-X software. The PSD tool revealed that the GL-3 sample was the most effective gamma photon attenuator, with half-value layer (HVL) values ranging from 0.002 to 3.706 cm. In addition, the Makishima and Mackenzie modeling was used to evaluate the mechanical and acoustic properties of these glasses, and the results of this study showed that the GL-3 glass samples exhibit excellent performance in terms of gamma photon attenuation, mechanical robustness, and acoustic properties.

Silicate glass is commonly used in commercial eyewear due to its ease of fabrication and good visibility (Albarzan et al., 2021). However, its processing temperature is high, and relatively few studies have been conducted on Gd-containing silicate glass-based radiation protection materials. A promising approach involves combining boron oxide (B_2O_3) and silicon dioxide (SiO_2), with B-O and Si-O bonds forming a stable non-uniform network, making the borosilicate glass system superior to both borate and soda-lime glasses. Mhareb (2023) synthesized four borosilicate glass samples using the melt-cooling method, transforming them into glass ceramics under heat treatment. The radiation shielding properties of these samples were evaluated, and it was found that replacing B_2O_3 with Gd_2O_3 improved both the neutron and radiation shielding properties. For instance, the FNRCS (Fast Neutron Removal Cross-Section) of BSTSGd0.5, BSTSGd1, BSTSGd1.5, BSTSGd1.5, and BSTSGd2 were 0.103, 0.105, 0.105, and 0.105 cm^{-1}, respectively. However, the addition of Gd_2O_3 was found to reduce the shielding performance for charged particles, indicating that the contribution of heavy elements to charged particle shielding is limited. Bawazeer and Sadeq (2023) doped the borosilicate glass system with Gd oxide (Gd_2O_3), sodium oxide (Na_2O), and iron oxide (Fe_2O_3). The study showed that the glass system's transparency increased with the addition of Gd_2O_3, and the final morphology is shown in Figure 6a. As illustrated in Figures 6b, c, with the increasing addition of Gd_2O_3, the density and optical bandgap of the glass sample increased. This resulted in a decrease in both the linear and nonlinear refractive indices, improved transparency, and a significant enhancement in radiation shielding performance. Consequently, this glass sample is a suitable candidate for high-transparency radiation shielding applications.

Compared to the extensive research on borate and silicate glass systems, there are relatively few studies on radiation shielding materials based on rare earth element Gd-doped phosphate, tellurite, and germanate glass systems. Phosphates, as conventional glasses, typically exhibit relatively poor chemical durability and require improvements through the addition of different oxides to enhance their service life (Saudi et al., 2020; Alalawi et al., 2022). In 2018, Tao Yu (2018) prepared a series of x Gd_2O_3-(50-x)BaO-50P_2O_5 ($0 \leq x \leq 7$ mol%) glass samples using the melt quenching method and irradiated them with a^{60}Co irradiation source. The results revealed the formation of brown phosphorus-oxygen hole centers (class I color centers) under γ-ray irradiation. The number of color centers decreased with increasing Gd_2O_3 content in the glass, indicating that Gd_2O_3 enhances the resistance to γ-irradiation in barium phosphate glass without introducing new structural units into the microscopic network.

The tellurite glass system has a lower processing temperature than silicates. However, the high dispersion coefficient and weak mechanical properties of tellurites limit their development in the optical field. Furthermore, tellurium is toxic, posing long-term

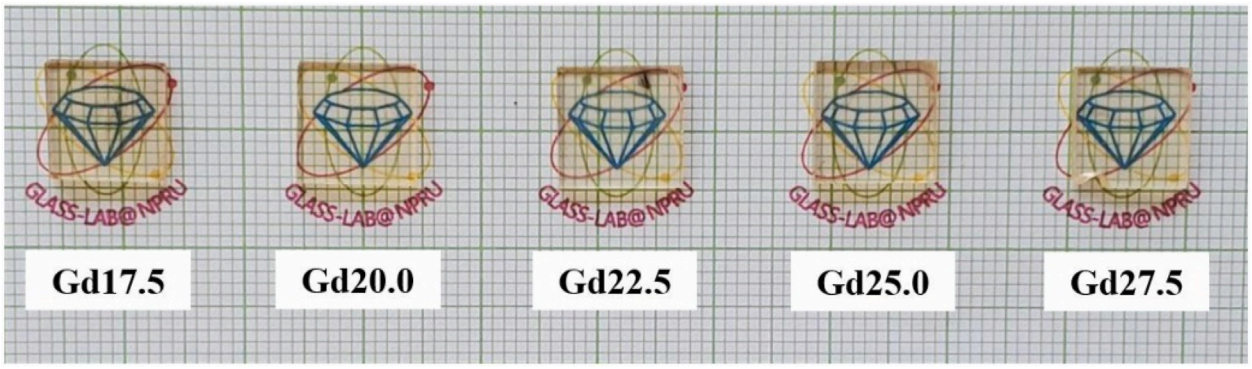

FIGURE 5
Photographic image of WGB glass sample (Kaewnuam et al., 2022).

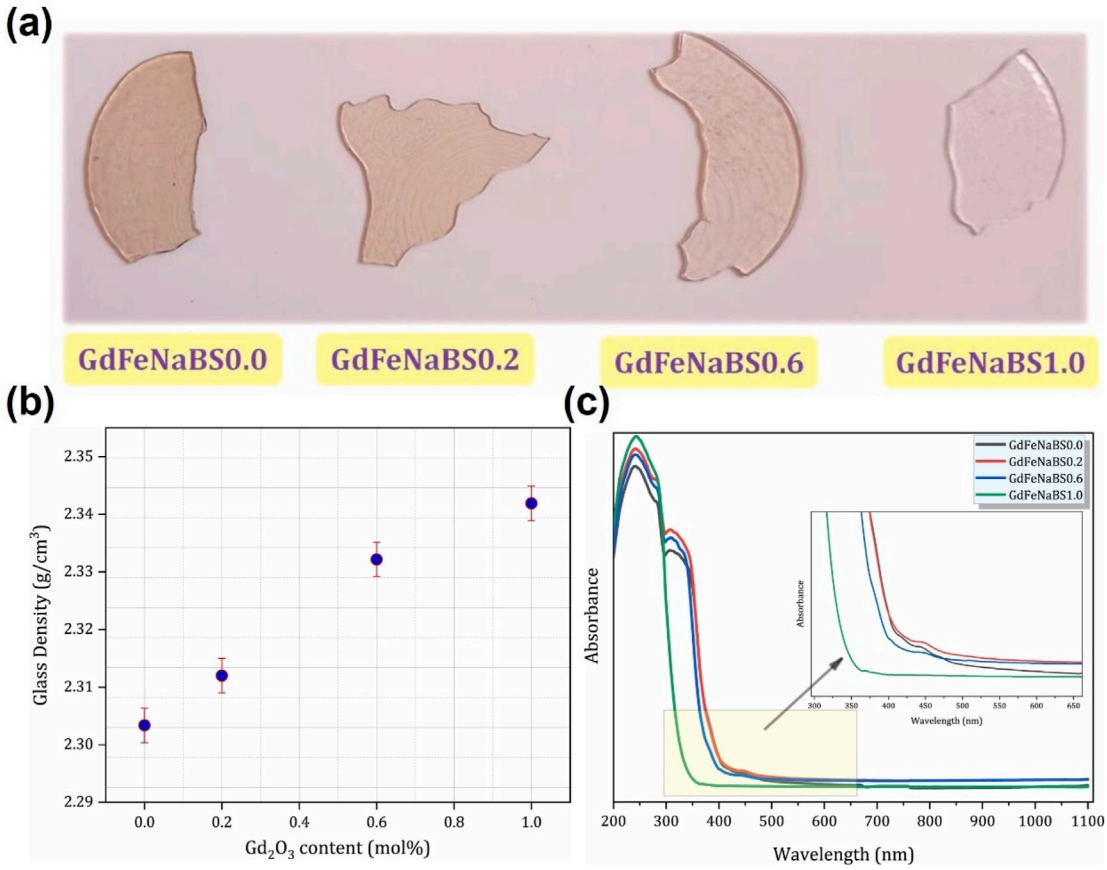

FIGURE 6
(a) Photographic image of the prepared GdFeNaBS glass sample, **(b)** dependence of GdFeNaBS glass sample on Gd_2O_3 Content (at room temperature), **(c)** absorbance of the prepared glass sample in the 200–1,100 nm UV-Visible-NIR range as a function of wavelength (Bawazeer and Sadeq, 2023).

health hazards to humans (Floressy Juhim et al., 2022; Mhareb et al., 2024). Al-Hadeethi and Agar (2020) employed software to assess the photon attenuation of the TeO_2-ZnO-Nb_2O_5-Gd_2O_3 glass system. The addition of ZnO as a network modifier improved the medium's opacity, fusion properties, chemical durability, and nonlinear refractive index. Incorporating niobate (Nb_2O_5) into the glass matrix stabilizes the network and may enhance the dual properties of the glass, serving both as a modifier and a network-forming agent. Gd_2O_3-doped glass matrices are highly efficient scintillator materials due to the efficient energy transfer from Gd^{3+} ions to activators. This makes them suitable for radiation detection and high-energy particle applications. The results showed that the

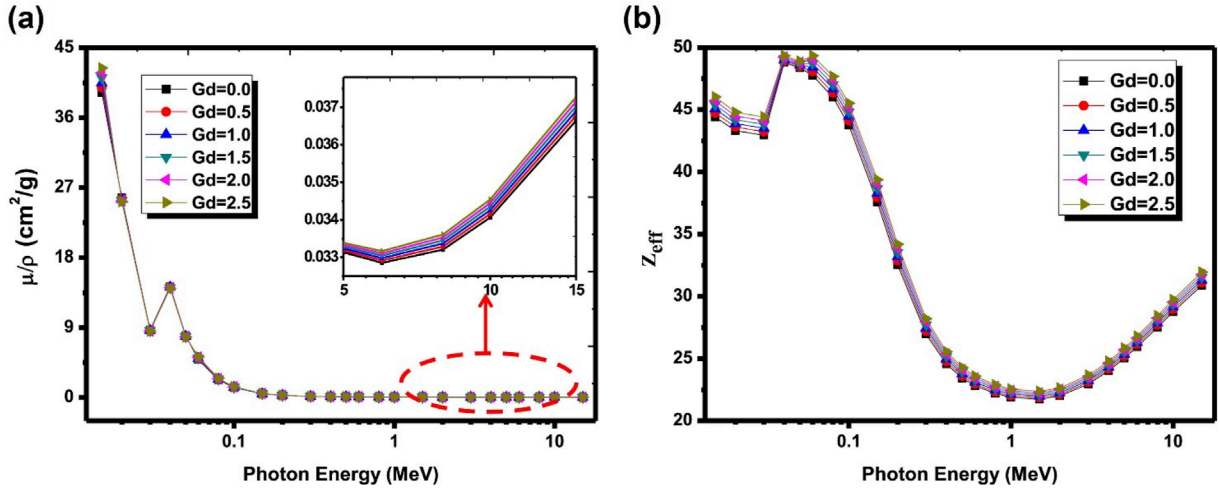

FIGURE 7
(a) Mass attenuation coefficient of TeO_2-ZnO-Nb_2O_5-Gd_2O_3 glass in the energy range of 0.015–10 MeV, **(b)** Effective atomic number of TeO_2-ZnO-Nb_2O_5-Gd_2O_3 glass (Al-Hadeethi and Agar, 2020).

attenuation capacity of ionized photons increased with the sample's density, indicating that high-density samples are needed for superior attenuation. As shown in Figure 7, the mass attenuation coefficient and effective atomic number of the tellurite glass were higher than those of the other samples when the Gd_2O_3 content was 2.5 mol%. Germanate glass offers good thermal stability, transparency, and a low melting point. However, germanium is a rare metal with limited availability, making germanate glass expensive to produce. As a result, it is generally used for specific optical components and lasers (Sayyed et al., 2019). Kawa and Kaky (2024) investigated photon energies ranging from 0.015 to 10 MeV in the B_2O_3-GeO_2-Eu_2O_3-R_2O_3 (where R = Y, La, and Gd) germanate glass system for its shielding capabilities. The results showed that the addition of elements with high atomic numbers (Z) effectively enhanced the photon attenuation of germanate glass.

2.3 Gd-containing ceramic-based composite shielding materials

Ceramic materials are a class of non-metallic inorganic compounds, typically prepared through high-temperature sintering or melting processes. These materials are known for their exceptional thermal stability and low conductivity, making them promising candidates for thermal insulation applications in reactors (Lo et al., 2015; Zhang and Bai, 2019; Zhang, 2021). The development of ceramic-based materials with neutron-shielding properties has become a significant area of research. Over recent decades, scholars specializing in nuclear materials have increasingly focused on ceramic-based systems due to their advantages, including high-temperature resistance, mechanical robustness, and tunable compositions (Oto et al., 2019).

Aluminum oxide ceramics (Al_2O_3) are widely used as carriers for electronic components because of their high hardness, high-temperature resistance, and high electrical insulation (Ghasemi-Kahrizsangi et al., 2017; Wu et al., 2024). However, its high sintering temperature and poor thermal conductivity limit the development of his application (Wu and Yu, 1988). Many researchers have reduced the sintering temperature by adding additives such as MgO and SiO_2 to Al_2O_3 ceramics to induce liquid-phase sintering (Wu and Yu, 1988; Lee et al., 2015; Zeng et al., 2022). Gradually, it has been found that the addition of rare earth elements can effectively reduce the sintering temperature and improve the mechanical properties of ceramic materials while preventing radiation damage to components (Ge et al., 2016). Ge et al. (2016) prepared Gd_2O_3/Al_2O_3 ceramic composites with different Gd_2O_3 contents by pressureless sintering methods using MgO and SiO_2 as additives. It was found that the addition of a small amount of Gd_2O_3 could promote the generation of spinel and olivine from MgO, SiO_2, and Al_2O_3, which greatly improved the properties of the ceramics, and the flexural strength and thermal conductivity of Gd_2O_3/Al_2O_3 ceramic composites added with 5 wt% Gd_2O_3 increased by 38.03 MPa and 8.95 W/(m·K). Tests using a highly active Co-60 source with a dose rate of 1.5 kGy/h revealed that the shielding rate of the composites against Co-60 γ-ray radiation increased with the addition of Gd_2O_3, and they also exhibited good mechanical stability under continuous γ-ray irradiation.

Boron-based ceramics can be synthesized at relatively low temperatures and are well-suited for radiation shielding applications due to the neutron absorption capacity of B. Dong et al. (2021) reported the development of $GdBO_3$ ceramics, which exhibit effective neutron shielding properties and low thermal conductivity, making them ideal multifunctional insulating materials. These bulk $GdBO_3$ ceramics were prepared for the first time via a simple solid-phase method. As the sintering temperature and boric acid content increased, the apparent porosity decreased, while the average pore size increased. The thermal conductivity of the ceramics ranged from 0.12 to 0.68 W/(m·K). The addition of boric acid improved the mechanical properties of the samples over various temperature ranges. The neutron shielding permeability of the samples with varying thicknesses was also evaluated, revealing that the neutron transmittance decreased with increased sample

thickness. The macroscopic cross-section of the material was found to be at least 0.641 cm^{-1}, which is promising for use in nuclear reactors. Aluminum borate ($Al_{18}B_4O_{33}$) is a binary compound that exhibits optimal refractory properties within the Al_2O_3-B_2O_3 phase diagram. It is considered a promising reinforcing agent and high-temperature structural material, particularly for its exceptional neutron shielding properties (Yu et al., 2016; Hernández et al., 2023). Li et al. (2021) synthesized Gd_2BO_3-$Al_{18}B_4O_{33}$ (GACCs) composite ceramics using $2Al_2O_3{\cdot}B_2O_3$ and α-Al_2O_3 as raw materials and Gd_2O_3 as a neutron shielding agent via pressureless sintering. To further explore the effects of the *in-situ* formation of $GdBO_3$ on the microstructure and mechanical properties of GACCs, the authors conducted experiments, including crystal morphology observation and thermal shock testing. As shown in the SEM images in Figure 8, the samples without added Gd_2O_3 showed no distinct areas, indicating that the etching treatment effectively removed the sintering agent Bi_2O_3. At higher magnification, numerous rod-like particles with a three-dimensional interlocking network structure were observed. As the Gd_2O_3 content increased, the distribution area of the bright regions expanded, and the directionality of the interlocking network became more pronounced. The formation of excess $GdBO_3$ led to intergranular microcracks, which could negatively impact the structural stability of the GACC. However, the thermal shock test revealed that a moderate amount of Gd_2O_3 did not adversely affect the structural stability of the composite, enhancing its mechanical and thermal properties. The lowest porosity observed for the composite was 1.8%, and the highest neutron shielding efficiency of 82.8% was achieved for the G12 probe sample.

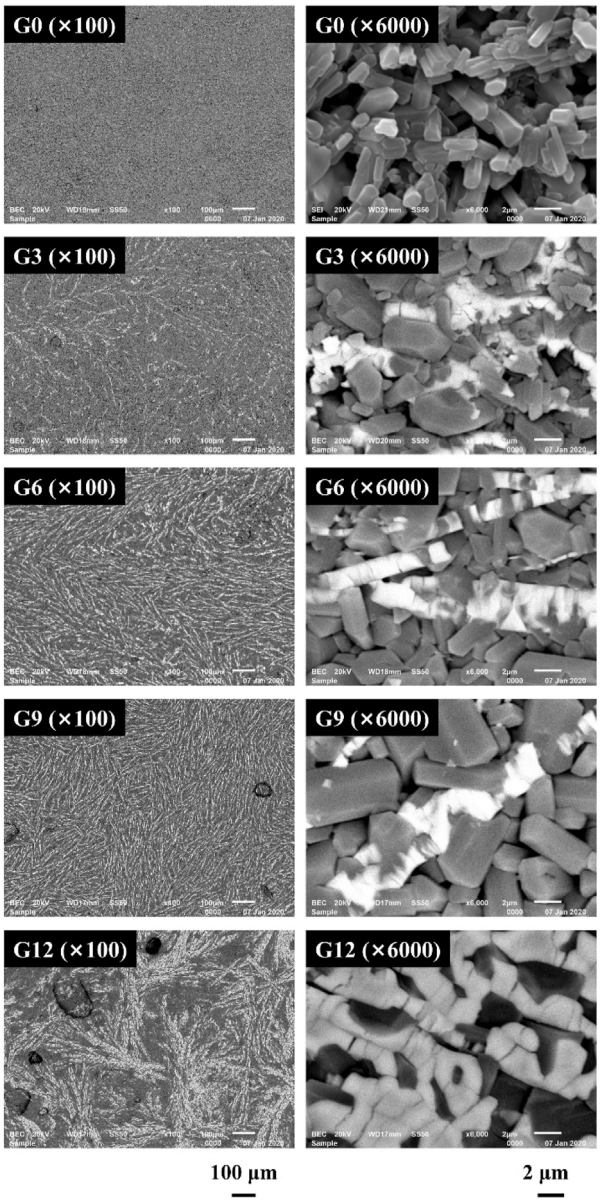

FIGURE 8
Crystal morphology of GACCs treated for 3 hours at 1,400°C (Li et al., 2021).

In 2015, the efficacy of entropy stabilization in oxide mixtures was demonstrated (Oses et al., 2020b). Inspired by high-entropy alloys, high-entropy disordered ceramics emerged, with ongoing research stimulating the incorporation of additional components to achieve a diverse range of physical and chemical properties. These materials are now used in various applications, including thermal barrier coatings, thermoelectrics, catalysts, batteries, and wear- and corrosion-resistant coatings (Oses et al., 2020a; Toher et al., 2022; Li Y. et al., 2024; Ward et al., 2024). To develop a material capable of absorbing both neutrons and gamma rays, Zhang et al. (2021) prepared a novel single-phase $(La_{0.2}Ce_{0.2}Gd_{0.2}Er_{0.2}Tm_{0.2})_2(WO_4)_3$ ceramic. The synthesis of this phase-pure rare-earth tungstate-based high-entropy ceramic (HEC) powder, based on tungstates known for their enhanced neutron absorption capacity, and its phase stability enhanced by the high-entropy effect, renders the powder less susceptible to failure under radiation. The ceramic powder was then uniformly mixed with epoxy resin (EP). In terms of thermal neutron shielding, the composite with the highest HEC content (EP/W_3) exhibited a shielding efficiency of nearly 100%, compared to approximately 50% for pure EP. For γ-ray shielding, the composite demonstrated a lead equivalent value at 65 keV that exceeded that of EP, indicating its effectiveness in shielding γ-rays in both low- and medium-energy regions.

Despite the rapid development of ceramic matrix composites for nuclear radiation shielding, the fabrication of ceramic materials presents challenges, including the need for high-temperature sintering, which complicates their production. Additionally, the brittleness of ceramics imposes limitations on the design of micro-mechanisms and compositions for practical applications. As the range of potential applications for shielding materials continues to grow, the fabrication requirements are becoming increasingly complex. The advent of 3D printing (3DP) technology provides new possibilities for the customized fabrication of intricate structures. As shown in Figure 9, Wang et al. (2022) employed DLP 3D printing to prepare Gd_2O_3 ceramics. The phase transition of Gd_2O_3 from cubic to monoclinic enhances the densification of sintered specimens, improving their mechanical properties. The authors fabricated lattices comprising numerous lattice elements and sintered them at various temperatures. The bending stress and bending elastic modulus of the sintered specimens at 1,600°C were found to be as high as 40 MPa and 20.219 GPa, respectively. These findings support the practical application of the material for neutron absorption and

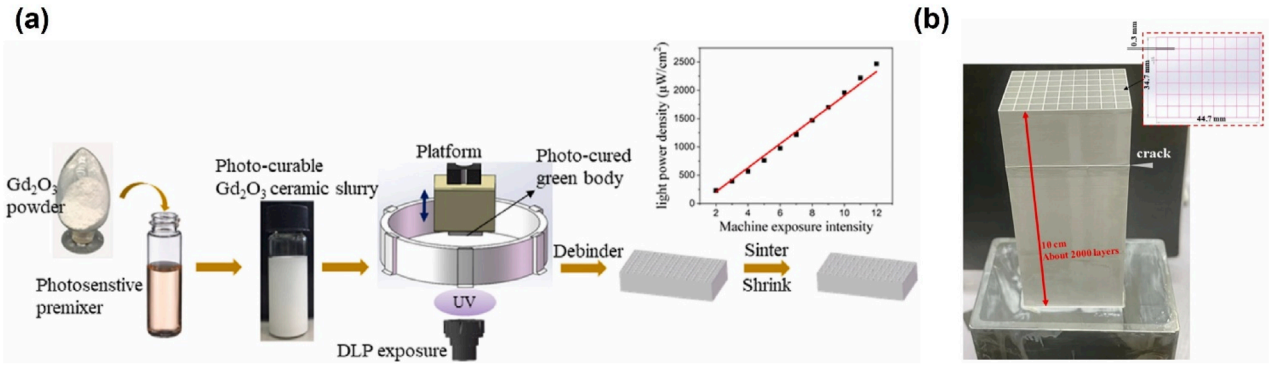

FIGURE 9
(a) schematic diagram of the Gd_2O_3 ceramic DLP-3DP process, **(b)** preparation of a 10 cm long lattice body and its cross-sectional image (Wang et al., 2022).

shielding, addressing the issue of constrained ceramic structures in confined environments. This research provides a foundation for future studies in this practical area.

2.4 Gd-containing polymer-based composite shielding materials

Metal matrix composites are characterized by high density, high cost, and processing challenges. Additionally, they are prone to corrosion under high-intensity irradiation, which can lead to the formation of cracks, cavities, and other defects, making them unsuitable for use in protective devices or miniaturized nuclear power plant applications. Glass-based composite materials, known for their high light transmission, are mainly utilized for visualizing operating equipment. Ceramic-based composite shielding materials, while offering high performance, exhibit brittleness and are difficult to process, significantly limiting their applicability under specific dynamic loading conditions.

Polymer-based radiation shielding materials are composed of polymers with high hydrogen content as the base material and substances with high and medium absorption cross-sections as additives. These additives, such as B and Gd, are particularly effective at absorbing thermal neutrons. Effective neutron shielding is achieved through three primary mechanisms: slowing down high-energy neutrons by hydrogen, scattering, and absorption by specific elements. Polymer-based materials offer excellent thermal stability, electrical insulation, and mechanical properties, along with advantages such as light weight and ease of processing. These characteristics make them ideal for use in confined or motorized environments and allow for a wide range of potential applications across multiple fields (Kim, 2023; Zhang et al., 2023; Alkarrani et al., 2024).

Polyethylene (PE) is known for its good chemical resistance, stability, lightweight nature, small size, and low processing cost. Additionally, PE contains many hydrogen atoms, which can effectively slow down neutrons and reduce their energy during collisions. However, its shielding effect on high-energy neutrons (fast neutrons) is relatively weak. To improve the shielding and mechanical properties of polyethylene, inorganic functional fillers with a high neutron-absorbing cross-section, such as Gd, are added to the polyethylene matrix. İrim et al. (2018) first used a fusion composite method to prepare new multifunctional neutron shielding materials based on high-density polyethylene (HDPE), incorporating nano-h-BN and nano-Gd_2O_3 as hybridized particles. The neutron and γ-ray transmittance of h-BN/Gd_2O_3/HDPE nanocomposites were compared with varying nanoparticle content. The results showed that Gd, a heavy element, exhibits a dual shielding effect on both gamma rays and neutrons. The neutron and γ-ray transmittance decreased with increasing h-BN and Gd_2O_3 concentrations, and some samples achieved shielding rates of around 80%–90% at low thicknesses. However, inorganic fillers tend to agglomerate and have poor interfacial compatibility in the polymer matrix, which can reduce the mechanical properties and impact the overall shielding performance of the composites (Hsieh et al., 2016; Shah et al., 2016). Surface modification of the fillers is an effective strategy to improve the compatibility of inorganic-organic interfaces (Wang et al., 2015; Zhong et al., 2020). Huo et al. (2021) used 3-(trimethoxysilyl)propyl methacrylate as a coupling agent to modify the surface of micro- and nano-Gd_2O_3, and prepared four lead-free composites using the hot pressing method: micro-Gd_2O_3/B_4C/HDPE, M-micro-Gd_2O_3/B_4C/HDPE, nano-Gd_2O_3/B_4C/HDPE, and M-nano-Gd_2O_3/B_4C/HDPE. The results showed that the composite containing 10 wt% M-nano-Gd_2O_3/20 wt% B_4C/70 wt% HDPE exhibited a higher initial decomposition temperature (T5%) of 463.5°C and a peak heat absorption temperature (TP) of 137.2°C. The tensile strength (19.6 MPa) was also significantly higher than that of pure HDPE (15.8 MPa). These findings demonstrate that the composite has excellent thermal stability and mechanical properties. The surface modification of the filler significantly enhanced the interfacial compatibility and dispersion of the filler within the polyethylene matrix, reducing stress concentration and improving the mechanical properties of the composites. Experimental measurements and Monte Carlo simulations were conducted to investigate the neutron and γ-ray shielding mechanisms of the composites. As shown in Figure 10, the composite containing 10 wt% M-nano-Gd_2O_3/20 wt% B_4C/70 wt% HDPE achieved 90% neutron shielding

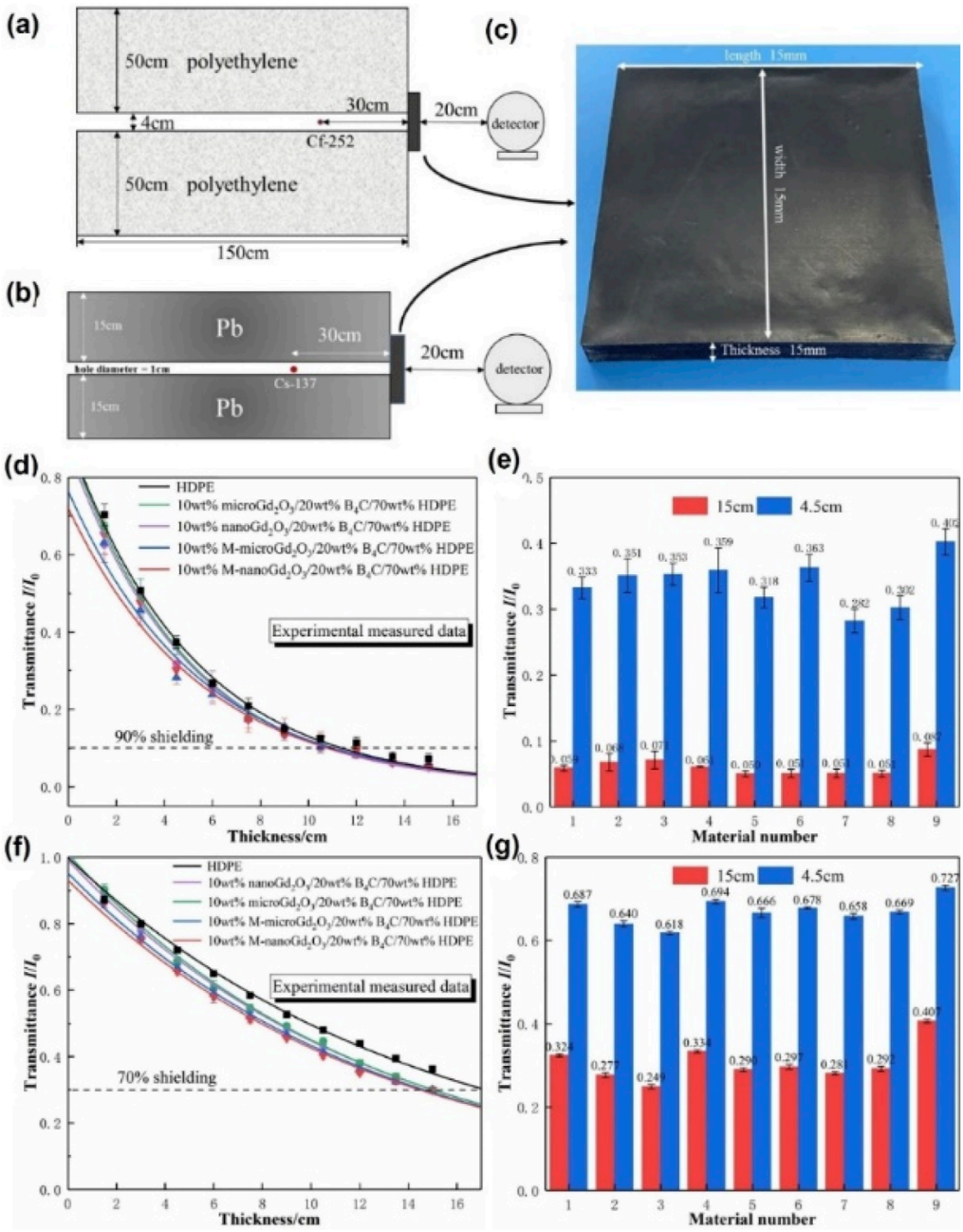

FIGURE 10
(a) Schematic diagram of the neutron radiation shielding experiment setup, **(b)** Schematic diagram of the gamma radiation shielding experiment setup, **(c)** Photograph of the composite materials, **(d)** Neutron flux attenuation of different composites composed of M-nanoGd_2O_3, M-microGd_2O_3, nanoGd_2O_3, and microGd_2O_3, **(e)** Comparison of neutron transmittance for different composites with thicknesses of 4.5 cm and 15 cm; **(f)** Gamma flux attenuation of different composites composed of M-nanoGd_2O_3, M-microGd_2O_3, nanoGd_2O_3, and microGd_2O_3,**(g)** Comparison of gamma photon transmittance for different composites with thicknesses of 4.5 cm and 15 cm (Huo et al., 2021).

at 9.1 cm in a Cf-252 environment and 70% gamma shielding at 13.7 cm in a Cs-137 environment, making it a promising material for neutron-gamma mixed-field radiation shielding.

Polyimide (PI) is less effective than polyethylene in neutron deceleration, but it boasts excellent thermal stability, chemical resistance, and radiation resistance, making it widely used in aerospace, precision electronic equipment, and high-temperature applications (Hu Xu et al., 2022; Xu et al., 2022; Li L. et al., 2024). Metal-organic frameworks (MOFs) are a class of porous materials consisting of metal ions or metal clusters linked to organic ligands by coordination bonds, and they have attracted significant attention due to their highly tunable pore structures and excellent chemical properties (García-Sánchez et al., 2017). Therefore, the combination of MOFs and polyimide (PI) holds great promise for developing new MOF/PI composites with enhanced mechanical properties and improved neutron shielding capabilities. Hu et al. (Hu et al., 2021)

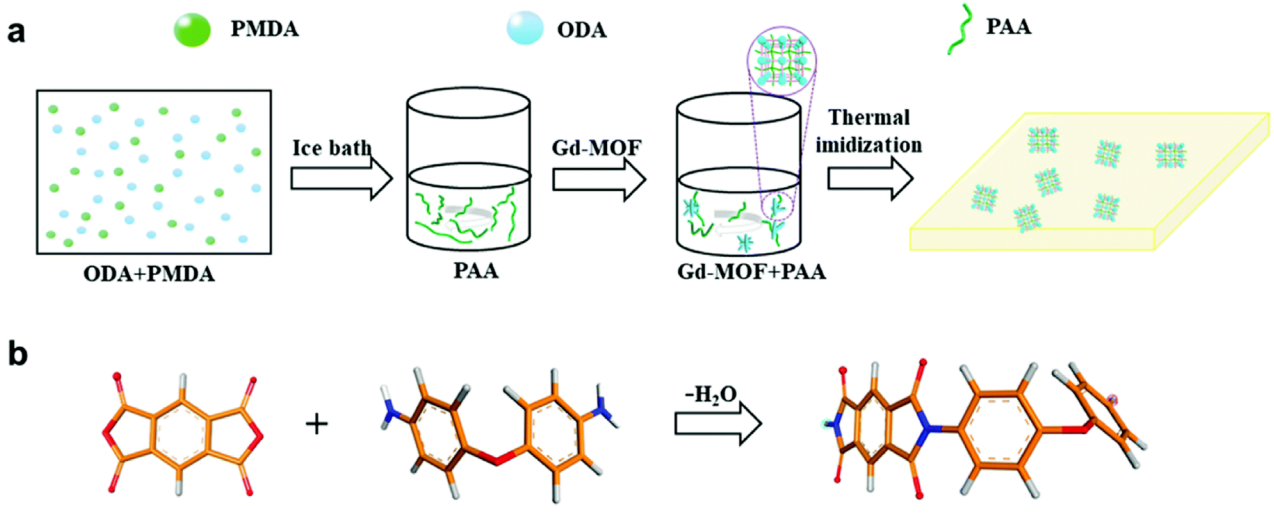

FIGURE 11
(a) Scheme of the process for the preparation of Gd-MOF/PI films, **(b)** Scheme of PI monomer. Color representation of different elements: o (red), c (orange), h (grey), n (blue) (Hu et al., 2021).

synthesized a rare-earth metal Gd-based metal-organic framework (Gd-MOF) from $GdCl_3$ and o-phenylene dimethyl dianhydride (PDMA) in N,N-dimethylformamide (DMF), as shown in the preparation process in Figure 11. The porous structure of Gd-MOFs provides a compatible interface with the PI substrate, facilitating effective interfacial load transfer. Scanning electron microscope (SEM) images revealed that the Gd-MOF/PI film containing 3 wt% filler had a smooth and flat surface without any noticeable matrix defects, indicating strong interfacial interactions between the filler and the PI matrix, resulting in excellent mechanical strength. The authors also performed shielding efficiency simulations using SuperMC. The results indicated that increasing the Gd-MOF content from 0 wt% to 20 wt% enhanced thermal neutron shielding ability but slightly reduced shielding effectiveness for fast neutrons. This trend is because hydrogen atoms slow down fast neutrons, and the reduction in hydrogen content diminishes the neutron-hydrogen atom interaction. Tan et al. (Tan et al., 2024) successfully synthesized $Gd_2O(CO_3)_2$@bismuth-based metal-organic frameworks (Bi-MOFs)/graphene nanoplates (GBG) composite fillers using a two-step hydrothermal method. These fillers were incorporated into a PMMA matrix at different mass percentages via a melt-blending and hot-pressing process. The study revealed that the addition of Gd significantly improved the gamma-ray shielding capacity of the GBG/PMMA composites, particularly for low-energy 59.5 keV gamma rays. The mass attenuation coefficient (MAC) of the GBG/PMMA-50 composite reached 2.70 cm^2/g, nearly 16 times higher than that of pure PMMA, greatly outperforming state-of-the-art materials in this category.

Simple physical blending does not allow for the formation of a dense shielding barrier in the polymer matrix, leading to the potential escape of neutrons through gaps between nanoparticles. Furthermore, some single shielding materials are ineffective across the entire range of neutron or gamma photon energies. To effectively shield both neutrons and gamma rays, researchers have designed structures to create dense barriers or achieve broad absorption. The overlapping of two-dimensional nanosheets has inspired many researchers. MXene, a new type of two-dimensional transition metal carbide or nitride with abundant polyhydroxy and negatively charged surfaces, presents itself as a promising substrate for grafting other materials (Li, 2023; Malaki and Varma, 2023). Zhu et al. (2022) successfully synthesized Gd@MXene nanosheets via a hydrothermal reaction and then prepared Gd@MXene/poly (vinyl alcohol) (PVA) thin films using a spin-coating process. The Gd@MXene nanosheets were randomly aligned to form-oriented, two-dimensional, fish-scale-like barrier walls in the films. These 2D fish-scale-like Gd@MXene barrier walls scatter neutron rays multiple times between the nanosheets, enhancing the neutron absorption efficiency of Gd atoms. This novel design, incorporating zero-dimensional Gd nanoparticles (NPs), not only improves neutron shielding performance but also provides valuable insights for the synthesis of advanced neutron shielding materials.

Bismuth oxide (Bi_2O_3) has been extensively studied as a functional filler due to its excellent γ-ray shielding properties (Tiamduangtawan et al., 2020a). However, it has weak shielding capabilities in the 36.4–90.5 keV energy range, limiting its effectiveness against low-energy gamma rays (Wei et al., 2023). In 2023, Wei et al. (2023) addressed this limitation by constructing heterostructures of Gd_2O_3 and Bi_2O_3. Using a simple two-step hydrothermal method, they synthesized heterostructured Bi_2O_3-$Gd_2O(CO_3)_2{\cdot}H_2O$ microscopic flowers, which were then incorporated into epoxy resin to form Bi_2O_3-$Gd_2O(CO_3)_2{\cdot}H_2O$/epoxy (EP) composites capable of shielding gamma rays across a broad energy range. The linear attenuation coefficients (LAC) of the heterostructured Bi_2O_3-$Gd_2O(CO_3)_2{\cdot}H_2O$/EP-30 composites at 59.5 keV, 661 keV, and 1.25 MeV were superior to those of the directly mixed Bi_2O_3-$Gd_2O(CO_3)_2{\cdot}H_2O$/EP-30 composites. The interaction of dielectric (661 keV) and high-energy (1.25 MeV) gamma

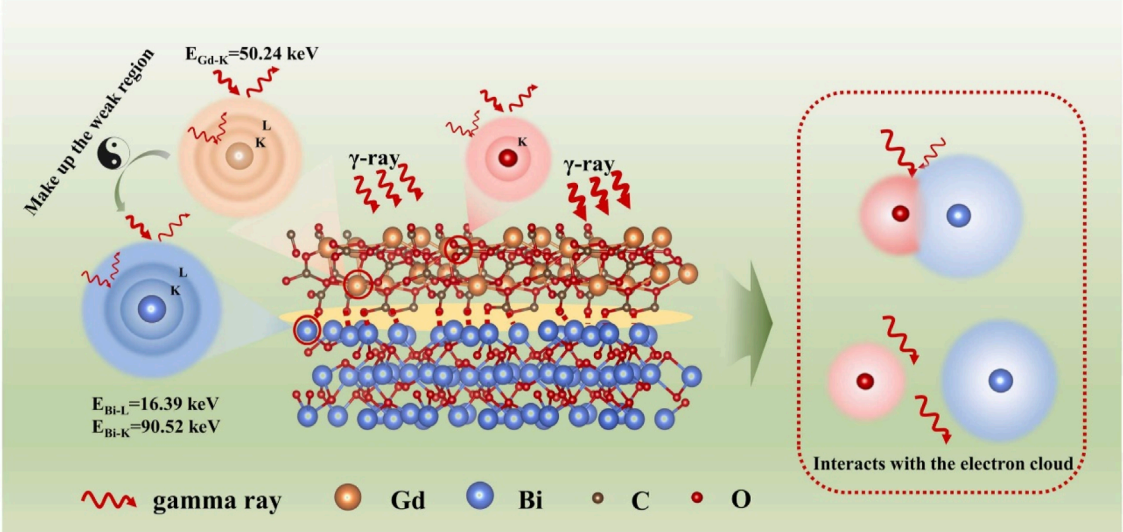

FIGURE 12
Mechanism of interaction of γ-rays with Bi_2O_3-$Gd_2O(CO_3)_2 \cdot H_2O$ non-homogeneous materials (Wei et al., 2023).

rays with the materials primarily occurs through Compton scattering. In contrast to simple co-mingling, new Bi-O bonds are formed at the heterogeneous interfaces, leading to electronic rearrangements, an increase in local electron density, and overlapping of the electron clouds (Figure 12). This overlap increases the probability of gamma rays colliding with outermost electrons, greatly enhancing Compton scattering. The construction of heterogeneous structures could become an effective method for designing radiation shielding materials. However, the impact of inhomogeneous interfaces on radiation shielding performance remains underexplored and requires further investigation.

As application scenarios evolve, composite components made from traditional matrices are often inflexible, brittle, and prone to fracture. As a result, researchers have focused on developing polymer-based composite shielding materials that meet more stringent requirements, such as high toughness, high strength, and the ability to effectively attenuate neutrons. These materials must also be capable of self-repair to extend their service life and reduce manufacturing costs. Polyvinyl alcohol (PVA) stands out due to its high mechanical strength, abrasion resistance, oxygen barrier properties, solvent/oil/grease resistance, non-toxicity (biocompatibility), and high hydrogen content, which aids in neutron modulation and attenuation (Rashad et al., 2020; Bai et al., 2022; Bijanu et al., 2024). Tiamduangtawan et al. (Tiamduangtawan et al., 2020b) incorporated fillers (Sm_2O_3 or Gd_2O_3) at concentrations of 0%–3.5%, 7.0%, and 10.5% into PVA hydrogels. Their study found that the neutron shielding efficiency of Gd2O3/PVA hydrogels was slightly higher than that of Sm_2O_3/PVA hydrogels at the same filler content and thickness. Furthermore, the overall tensile properties of Gd_2O_3/PVA hydrogels were superior to those of Sm_2O_3/PVA hydrogels. Additionally, both Sm_2O_3/PVA and Gd_2O_3/PVA hydrogels exhibited self-healing properties at fractured surfaces (Figure 13). The recoverable strength of the hydrogels increased over time, making them suitable for use as substitutes for paraffin wax in transportation drums or as shielding biomaterials in medical diagnosis and radiotherapy. Poltabtim et al. (Poltabtim et al., 2022) developed Gd_2O_3/natural rubber (NR) composites by incorporating reversible ions into the NR network. These composites demonstrated effective shielding properties against neutrons and X-rays, as well as self-healing capabilities. The addition of Gd_2O_3 resulted in a decrease in I/I_0, half-value layer (HVL), and ten-value layer (TVL), while increasing the linear attenuation coefficient (μ), mass attenuation coefficient (μm), and lead equivalent (Pbeq) of the NR composites. These findings indicate that Gd_2O_3 is an effective filler for neutron and X-ray protection. After 60 min of self-repair, the recoverable strength and recovery values of the NR composites ranged from 0.30 to 0.4 MPa and 3.7%–9.4%, respectively. This self-repairing composite material can be used as a new type of radiation shielding material, which effectively attenuates neutrons and X-rays, prolonging the service life of protective materials and enhancing user safety. It also lays the foundation for the future development of "smart" shielding materials.

The Gd-containing polymer-based radiation shielding materials discussed above are summarized in Table 4. Currently, polymer-based composite shielding materials combine a variety of basic polymers (e.g., polyethylene, polyurethane, epoxy resin, polyvinyl alcohol, rubber) with different fillers (e.g., metal powders, hydrogen source materials) to achieve various shielding effects. Several innovative preparation methods, such as 3D printing and injection molding, have been explored, along with filler modification techniques. Moving forward, the development of polymer-based composite shielding materials will likely focus on multifunctionality, ecological sustainability, intelligence, and the application of nanotechnology to meet the increasingly complex demands of future applications.

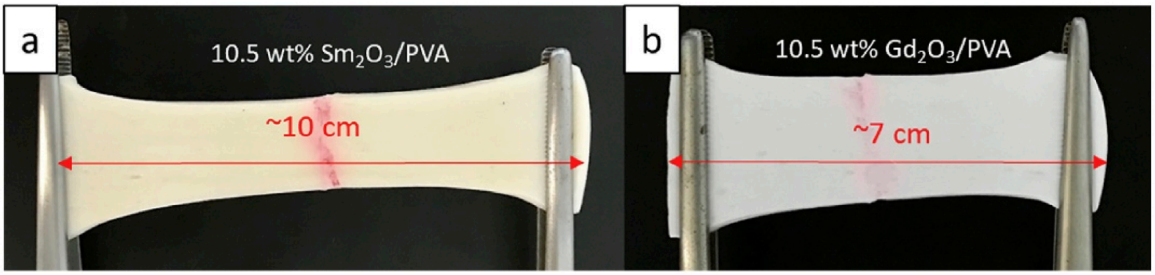

FIGURE 13
Self-healing images of **(a)** Sm_2O_3/PVA and **(b)** Gd_2O_3/PVA hydrogels stretched (original length of ~3.5 cm, healing time of 3 h). The red vertical deformation in the middle of the two samples indicates that the samples were cut and contacted for self-healing (Tiamduangtawan et al., 2020b).

TABLE 4 Gd-containing polymer matrix radiation shielding materials and their properties are discussed above.

Year	Composition	Gadolinium content	Shielding efficiency	Other properties	References
2018	h-BN/Gd_2O_3/HDPE	3wt%	Neutron shielding rate 80%–90% (2–5 cm)	h-BN	İrim et al. (2018)
2021	M-Gd_2O_3/B_4C/HDPE	10wt%	Neutron shielding rate 90% (9.1 cm) Gamma ray shielding efficiency 70% (13.7 cm)	Surface modification	Huo et al. (2021)
2021	Gd-MOF/PI	3wt%	Neutron shielding rate 90% (2 mm)	MOF	Hu et al. (2021)
2020	Gd_2O_3/PVA	3.5wt%	$\mu = 1.69cm^{-1}$ HVL = 4.1 mm TVL = 13.6 mm	Self-healing hydrogel	Tiamduangtawan et al. (2020b)
2022	Gd@MXene/PVA	20wt%	Neutron shielding rate 50% (80 μm)	Two-dimensional fish-scale structure	Zhu et al. (2022)
2023	Bi_2O_3-$Gd_2O(CO_3)_2$·H_2O/EP-30	5wt%	HVL = 0.72 cm $LAC = 3.49cm^{-1}$ (59.5 keV)	Heterostructure	Wei et al. (2023)
2022	Gd_2O_3/NR	50phr	HVL = 2.0 mm	Self-healing	Poltabtim et al. (2022)
2024	$Gd_2O(CO_3)_2$@Bi-MOF/graphene nanoplatelets (GBG)-PMMA	—	MAC = 2.70 cm^2/g	^{222}Rn and gamma-ray shielding performance	Tan et al. (2024)

3 Conclusion and outlook

Existing research programs have successfully achieved effective radiation shielding across different radiation sources and doses. Shielding materials have evolved from traditional options such as heavy metals, concrete, water, lead, and graphite, and have gradually transitioned to composite materials known for their lightweight, high efficiency, and overall excellent performance. While these traditional materials are still commonly used in fields like reactor radiation protection due to their low cost and ease of large-scale production, they come with significant disadvantages, including high weight, toxicity, and poor stability. As a result, researchers have focused on improving the shielding performance of these materials while aiming to reduce their weight and cost. Composite materials offer notable advantages in neutron shielding, including their lightweight nature, ease of molding, variety, and tunable performance. Through thoughtful component design, composites can effectively absorb and scatter neutrons, reducing the structural burden compared to traditional heavy metals. Additionally, composites are flexible and customizable, allowing for designs tailored to specific needs. Some of these materials are made from environmentally friendly raw materials, helping to minimize their environmental impact. These characteristics have made composites increasingly attractive for applications in nuclear energy, medicine, and industry.

The rare earth element gadolinium (Gd) stands out due to its high atomic number, large neutron absorption cross-section, and low intensity of neutron radiation. Gd effectively compensates

for the weak absorption of low-energy rays by heavy metals like lead, thus reducing the biological toxicity associated with lead. As a result, Gd composites with other materials exhibit excellent performance in radiation shielding. This paper focuses on Gd-containing composite shielding materials, which include metal-based, glass-based, ceramic-based, and polymer-based composites. Each material type is employed in different fields based on its unique advantages. Metal matrix composites are known for their high strength and excellent thermal conductivity, making them ideal for radiation shielding in high-intensity and high-temperature environments. Glass matrix composites are lightweight, highly transparent, and corrosion-resistant, making them suitable for use in visualization equipment. Ceramic matrix composites, with their superior radiation, high temperature, and wear resistance, are well-suited for harsh environments. Polymer matrix composites are valued for being lightweight, flexible, and cost-effective, making them ideal for electronic equipment protection, aerospace, medical devices, and other applications. However, as nuclear energy use continues to grow and application opportunities diversify, radiation-shielding composite materials still face several challenges that need to be addressed:

(1) Lack of universal solutions for filler dispersion in polymer-based composites. In polymer-based composite shielding materials, inorganic fillers are prone to agglomeration within the matrix. Excessive doping can impede the material's shielding, thermal, mechanical, and other properties. When the filler is dispersed uniformly within the matrix, the probability of composite material collisions with radiation or particles increases significantly, enhancing shielding performance. Furthermore, filler agglomeration can also result in stress concentration, decreased interfacial adhesion with the matrix, and a reduction in the mechanical strength and toughness of the composite material. Future studies should prioritize scalable, matrix-agnostic dispersion techniques (e.g., adaptive interfacial design, stimuli-responsive nanoparticle alignment) while maintaining shielding efficiency and mechanical stability.

(2) Incomplete mitigation of secondary radiation risks. Gd has significant advantages in neutron shielding, especially its isotope Gd-157, which has an extremely high neutron trapping capacity, enabling it to effectively reduce neutron radiation. After absorbing neutrons, these elements may be transformed into other unstable isotopes. These unstable isotopes undergo secondary radioactive decay to produce gamma rays or beta particles, which is known as secondary radiation. Therefore, Gd-containing composite shielding materials must be prepared in conjunction with other elements that can absorb gamma rays, or appropriate protection and measures must be taken to ensure safety and effectiveness.

(3) Limited innovation in cost-effective Gd utilization. Gd is a rare metal with relatively limited resources, and the costs associated with mining and processing Gd, and its alloys are relatively high, which has thus far precluded large-scale use. The key challenges currently facing the development of Gd-containing composite shielding materials are improvements to the production process, increased processing efficiency and utilization rate of Gd, and reductions in production costs.

(4) Incomplete mitigation of secondary radiation risks. Currently, composite shielding materials can only provide effective shielding under a single application scenario. As the complexity of shielding materials continues to increase, the comprehensive performance requirements of these materials are also becoming more demanding. Consequently, materials must be capable of achieving a variety of functionalities to meet the evolving needs of their applications.

The unique physicochemical properties of gadolinium (Gd) as an effective radiation absorber provide it with a significant advantage in shielding applications. With continued advancements in science and technology, Gd-containing composites are expected to evolve into more sophisticated products. This will be accomplished by integrating sensing technology with adaptive properties through the application of nanotechnology and advanced composite fabrication techniques. Additionally, the development of lightweight, temperature-resistant, mechanically robust, and environmentally friendly composites will promote their widespread use in areas such as medical imaging, nuclear energy safety, and aerospace, effectively addressing the increasingly complex demands for radiation protection.

Author contributions

JC: Conceptualization, Methodology, Writing–original draft. XZ: Conceptualization, Investigation, Methodology, Writing–original draft. WX: Formal Analysis, Writing–original draft. DP: Conceptualization, Methodology, Writing–review and editing. WW: Funding acquisition, Investigation, Methodology, Writing–review and editing.

Funding

The author(s) declare that financial support was received for the research and/or publication of this article. The authors thank the financial support from Research and Development Project on New Multifunctional Lightweight Neutron and Gamma-Ray Composite Shielding Materials for Yangjiang Nuclear Power Plant.

Conflict of interest

Authors JC, XZ, and WX were employed by Yangjiang Nuclear Power Co. Ltd.

The remaining authors declare that the research was conducted in the absence of any commercial or financial relationships that could be construed as a potential conflict of interest.

Generative AI statement

The author(s) declare that no Generative AI was used in the creation of this manuscript.

Publisher's note

References

Abou Hussein, E. M., and Madbouly, A. M. (2024). Fabrication and characterization of different PbO borate glass systems as radiation-shielding containers. *Sci. Rep.* 14 (1), 2638. doi:10.1038/s41598-024-52071-x

Alalawi, A., Eke, C., Alzahrani, N. j., Alomairy, S., Alsalmi, O., Sriwunkum, C., et al. (2022). Attenuation properties and radiation protection efficiency of Tb_2O_3-La_2O_3-P_2O_5 glass system. *J. Aust. Ceram. Soc.* 58 (2), 511–519. doi:10.1007/s41779-022-00707-4

Albarzan, B., Hanfi, M. Y., Almuqrin, A. H., Sayyed, M. I., Alsafi, H. M., and Mahmoud, K. A. (2021). The influence of titanium dioxide on silicate-based glasses: an evaluation of the mechanical and radiation shielding properties. *Materials* 14 (12), 3414. doi:10.3390/ma14123414

Al-Buriahi, M. S., Tamam, N., Somaily, H. H., Alrowaili, Z. A., Saleh, H. H., Olarinoye, I. O., et al. (2022). Estimation of radiation protection ability of borate glass system doped with CdO, PbO, and TeO_2. *Radiat. Phys. Chem.* 193, 109996. doi:10.1016/j.radphyschem.2022.109996

Al-Buriahi, M. S., Tekin, H. O., Kavaz, E., Tonguc, B. T., and Rammah, Y. S. (2019). New transparent rare earth glasses for radiation protection applications. *Appl. Phys. A* 125 (12), 866. doi:10.1007/s00339-019-3077-8

Al-Hadeethi, Y., M.I., S., and Agar, O. (2020). Ionizing photons attenuation characterization of quaternary tellurite–zinc–niobium–gadolinium glasses using Phy-X/PSD software. *J. Non-Cryst. Solids* 538, 120044. doi:10.1016/j.jnoncrysol.2020.120044

Alharshan, G. A., Eke, C., Alrowaili, Z. A., ben Ahmed, S., Olarinoye, I. O., and Al-Buriahi, M. S. (2022). Influence of rare-earth ions on the radiation protection ability of some optical glasses containing Bi_2O_3 and SiO_2. *Optik* 264, 169371. doi:10.1016/j.ijleo.2022.169371

Alkarrani, H., Almisned, G., and Tekin, H. O. (2024). A benchmarking analysis on different rubber materials: towards customisation of lightweight and effective radiation protection solutions for aerospace and electronic applications. *J. Rubber. Res.* doi:10.1007/s42464-024-00272-4

Almousa, N., Boudaghi Malidarreh, R., Issa, S. A. M., and Zakaly, H. M. H. (2024). Synergistic effects of Gd_2O_3 and SiO_2 in enhancing the acoustic, mechanical, and shielding qualities of borate glasses. *Radiat. Phys. Chem.* 224, 112060. doi:10.1016/j.radphyschem.2024.112060

An, J., Qu, Y., and Wang, G. (2023). The multiple roles of rare earth elements in the field of photocatalysis. *Inorg. Chem. Front.* 11 (1), 11–28. doi:10.1039/d3qi02006a

Anishur Rahman, A. T. M., Vasilev, K., and Majewski, P. (2010). Ultra small Gd_2O_3 nanoparticles: absorption and emission properties. *J. Colloid Interface Sci.* 354 (2), 592–596. doi:10.1016/j.jcis.2010.11.012

Bai, H., Li, Y., Zhang, S., Ma, P., and Dong, W. (2022). Photo-crosslinkable poly (vinyl alcohol)/nanocrystalline cellulose composites with controllable performance and exceptional water vapor barrier property for packaging application. *Cellulose* 29, 7721–7734. doi:10.1007/s10570-022-04760-x

Bawazeer, O., and Sadeq, M. S. (2023). Compositional dependency of transparency, optical and radiation shielding parameters inside Gd_2O_3–Fe_2O_3–Na_2O–SiO_2–B_2O_3 glass. *Ceram. Int.* 50 (1), 159–173. doi:10.1016/j.ceramint.2023.10.079

Bijanu, A., Arya, R., Rajak, G., Gowri, V. S., Shil, R., Banerjee, K., et al. (2024). Flexible, chemically bonded bismuth/tungsten-based polyvinyl alcohol-polyvinyl pyrrolidone composite for gamma and neutron shielding application. *J. Appl. Polym. Sci.* 141 (22), 55435. doi:10.1002/app.55435

Biradar, S., Dinkar, A., Manjunatha, Bennal, A. S., Devidas, G. B., Hareesh, B. T., et al. (2024). Comprehensive investigation of borate-based glasses doped with BaO: an assessment of physical, structural, thermal, optical, and radiation shielding properties. *Opt. Mat.* 150, 115176. doi:10.1016/j.optmat.2024.115176

Boice, J. D., Cohen, S. S., Mumma, M. T., Hagemeyer, D. A., Chen, H., Golden, A. P., et al. (2022). Mortality from leukemia, cancer and heart disease among U.S. nuclear power plant workers, 1957–2011. *Int. J. Radiat. Biol.* 98 (4), 657–678. doi:10.1080/09553002.2021.1967507

Choi, Y., Baik, Y., Moon, B.-M., and Sohn, D.-S. (2016). Corrosion and wear properties of cold rolled 0.087% Gd lean duplex stainless steels for neutron absorbing material. *Nucl. Eng. Technol.* 48 (1), 164–168. doi:10.1016/j.net.2015.10.002

Choi, Y., Moon, B. M., and Sohn, D.-S. (2013). Fabrication of Gd containing duplex stainless steel sheet for neutron absorbing structural materials. *Nucl. Eng. Technol.* 45 (5), 689–694. doi:10.5516/net.07.2013.015

Cong, S., Ran, G., Li, Y., and Chen, Y. (2020). Ball-milling properties and sintering behavior of Al-based Gd_2O_3–W shielding materials used in spent-fuel storage. *Powder Technol.* 369, 127–136. doi:10.1016/j.powtec.2020.05.029

Do, M., Ramkissoon, A., Berriault, C., Villeneuve, P., and Demers, P. (2019). O6B.3 Risk of leukemia after chronic exposure to gamma radiation among ontario uranium miners? *Occup. Environ. Med.* 76 (Suppl. 1), A53.3–A54. doi:10.1136/oem-2019-epi.144

Dong, C., Li, Y., Li, S., Jia, W., Chen, R., Lao, D., et al. (2021). Thermally insulating $GdBO_3$ ceramics with neutron shielding performance. *Int. J. Appl. Ceram. Technol.* 19 (3), 1428–1438. doi:10.1111/ijac.13984

Dorenbos, P. (2013). Lanthanide 4f-electron binding energies and the nephelauxetic effect in wide band gap compounds. *J. Lumin.* 136, 122–129. doi:10.1016/j.jlumin.2012.11.030

Eman, E. B., Mahmoud, O. A. E.-M., Emad, A. E., Bahig, M. A., Karem, A. M., Lilly, H. K., et al. (2021). Lead–bismuth tungstate composite as a protective barrier against gamma rays. *Mat. Chem. Phys.* 275, 125262. doi:10.1016/j.matchemphys.2021.125262

Floressy Juhim, F. P. C., Awang, A., Duinong, M., Rasmidi, R., Rumaling, M. I., and Rumaling, M. I. (2022). Review—radiation shielding properties of tellurite and silicate glass. *ECS J. Solid State Sci. Technol.* 11, 076006. doi:10.1149/2162-8777/ac81ea

Fu, X., Ji, Z., Lin, W., Yu, Y., and Wu, T. (2021). The advancement of neutron shielding materials for the storage of spent nuclear fuel. *Sci. Technol. Nucl. Install.* 2021 (1), 1–13. doi:10.1155/2021/5541047

Gan, B., Liu, S., He, Z., Chen, F., Niu, H., Cheng, J., et al. (2021). Research progress of metal-based shielding materials for neutron and gamma rays. *Acta Metall. Sin. Engl. Lett.* 34 (12), 1609–1617. doi:10.1007/s40195-021-01259-5

García-Sánchez, A., Liras, M., Fresno, F., Barawi, M., Gutierrez-Puebla, E., Monge, Á., et al. (2017). Metal–organic frameworks based on conjugated organic ligands for optoelectronic applications. *Acta Crystallogr. Sect. A Found. Adv.* 73 (a2), c202. doi:10.1107/s2053273317093718

Gaylan, Y., and Avar, B. (2024). Al–B_4C-(Gd, Gd_2O_3) composite materials: synthesis and characterization for neutron shielding applications. *Nucl. Eng. Technol.* 56 (12), 5201–5211. doi:10.1016/j.net.2024.07.027

Ge, R., Zhang, Y., Liu, Y., Fang, J., Luan, W., and Wu, G. (2016). Effect of Gd_2O_3 addition on mechanical, thermal and shielding properties of Al_2O_3 ceramics. *J. Mat. Sci. Mat. Electron.* 28 (8), 5898–5905. doi:10.1007/s10854-016-6263-x

Gerward, L. (1999). Paul villard and his discovery of gamma rays. *Phys. Perspect.* 1, 367–383. doi:10.1007/s000160050028

Ghasemi-Kahrizsangi, S., Gheisari Dehsheikh, H., and Boroujerdnia, M. (2017). Effect of micro and nano-Al_2O_3 addition on the microstructure and properties of MgO-C refractory ceramic composite. *Mat. Chem. Phys.* 189, 230–236. doi:10.1016/j.matchemphys.2016.12.068

Glass, B. (1957). The genetic hazards of nuclear radiations. *Science* 126 (3267), 241–246. doi:10.1126/science.126.3267.241

Gupta, M. (2020). Metal matrix composites—the way forward. *Appl. Sci.* 10 (9), 3000. doi:10.3390/app10093000

Hernández, M. F., López, P. V., Ferrari, B., Rendtorff, N. M., and Sánchez-Herencia, A. J. (2023). Colloidal processing, sintering and properties of aluminum borate $Al_{18}B_4O_{33}$ porous ceramics. *Ceram. Int.* 50 (1), 1615–1622. doi:10.1016/j.ceramint.2023.10.255

Hidaka, H., Ebihara, M., and Yoneda, S. (2000). Isotopic study of neutron capture effects on Sm and Gd in chondrites. *Earth Planet. Sci. Lett.* 180 (1), 29–37. doi:10.1016/S0012-821X(00)00148-5

Ho, S. L., Yue, H., Tegafaw, T., Ahmad, M. Y., Liu, S., Nam, S.-W., et al. (2022). Gadolinium neutron capture therapy (GdNCT) agents from molecular to nano: current status and perspectives. *ACS OMEGA* 7 (3), 2533–2553. doi:10.1021/acsomega.1c06603

Hsieh, C.-T., Pan, Y.-J., Lou, C.-W., Huang, C.-L., Lin, Z. I., Liao, J.-M., et al. (2016). Polylactic acid/carbon fiber composites: effects of functionalized elastomers on mechanical properties, thermal behavior, surface compatibility, and electrical characteristics. *Fibers Polym.* 17, 615–623. doi:10.1007/s12221-016-5922-0

Hu, C., Huang, Q., and Zhai, Y. (2021). Thermal, mechanical investigation and neutron shielding analysis for Gd-MOF/polyimide materials. *RSC Adv.* 11 (63), 40148–40158. doi:10.1039/d1ra07500d

Hu, G., Shi, G., Hu, H., Yang, Q., Yu, B., and Sun, W. (2020). Development of gradient composite shielding material for shielding neutrons and gamma rays. *Nucl. Eng. Technol.* 52 (10), 2387–2393. doi:10.1016/j.net.2020.03.029

Hu, Z., Haneklaus, S., Sparovek, G., and Schnug, E. (2006). Rare earth elements in soils. *Commun. Soil Sci. Plant Anal.* 2, 1381–1420. doi:10.1080/00103620600628680

Huo, Z., Zhao, S., Zhong, G., Zhang, H., and Hu, L. (2021). Surface modified-gadolinium/boron/polyethylene composite with high shielding performance for neutron and gamma-ray. *Nucl. Mat. Energy* 29, 101095. doi:10.1016/j.nme.2021.101095

Hu Xu, D. L., Sun, W.-Q., Wu, R.-J., Liao, Wu, Li, X.-L., Hu, G., et al. (2022). Study on the design, preparation, and performance evaluation of heat-resistant interlayer-polyimide-resin-based neutron-shielding materials. *Materials* 15 (12), 2978. doi:10.3390/ma15092978

İrim, Ş. G., Wis, A. A., Keskin, M. A., Baykara, O., Ozkoc, G., Avcı, A., et al. (2018). Physical, mechanical and neutron shielding properties of h-BN/Gd_2O_3/HDPE ternary nanocomposites. *Radiat. Phys. Chem.* 144, 434–443. doi:10.1016/j.radphyschem.2017.10.007

Jayakumar, S., Saravanan, T., and Philip, J. (2023). A review on polymer nanocomposites as lead-free materials for diagnostic X-ray shielding: recent advances, challenges and future perspectives. *Hybrid. Adv.* 4, 100100. doi:10.1016/j.hybadv.2023.100100

Ji, B., Wang, D., Li, T., Xia, Y., Cao, F., Zhang, S., et al. (2024). Corrosion-resistant Gd particles-doped Fe-based amorphous coatings with excellent neutron absorption properties. *Corros. Sci.* 238, 112376. doi:10.1016/j.corsci.2024.112376

Jung, Y., Lee, M., Kim, K., and Ahn, S. (2020). $^{10}B(n, \alpha)^7Li$ reaction-induced gas bubble formation in Al–B_4C neutron absorber irradiated in spent nuclear fuel pool. *J. Nucl. Mat.* 533, 152077. doi:10.1016/j.jnucmat.2020.152077

Kaewnuam, E., Wantana, N., Tanusilp, S., Kurosaki, K., Limkitjaroenporn, P., and Kaewkhao, J. (2022). The influence of Gd_2O_3 on shielding, thermal and luminescence properties of WO_3–Gd_2O_3–B_2O_3 glass for radiation shielding and detection material. *Radiat. Phys. Chem.* 190, 109805. doi:10.1016/j.radphyschem.2021.109805

Kaur, P., Singh, D., and Singh, T. (2016). Heavy metal oxide glasses as gamma rays shielding material. *Nucl. Eng. Des.* 307, 364–376. doi:10.1016/j.nucengdes.2016.07.029

Kawa, M., and Kaky, M. I. S. (2024). Selected germanate glass systems with robust physical features for radiation protection material use. *Radiat. Phys. Chem.* 215, 111321. doi:10.1016/j.radphyschem.2023.111321

Kim, S.-C. (2023). Evaluation of shielding performance of gamma ray shielding tungsten polymer composite with LBL-type layered structure. *Coatings* 14 (1), 36. doi:10.3390/coatings14010036

Kregl, L., Wallner, G. M., Lang, R. W., and Mayrhofer, G. (2017). Effect of resin modifiers on the structural properties of epoxy resins. *J. Appl. Polym. Sci.* 134 (44). doi:10.1002/app.45348

Kursun, C., Gao, M., Yalcin, A. O., Parrey, K. A., and Gaylan, Y. (2024). Structure, mechanical, and neutron radiation shielding characteristics of mechanically milled nanostructured (100-x)Al-xGd_2O_3 metal composites. *Ceram. Int.* 50 (15), 27154–27164. doi:10.1016/j.ceramint.2024.05.013

Kurtulus, R. (2024). Recent developments in radiation shielding glass studies: a mini-review on various glass types. *Radiat. Phys. Chem.* 220, 111701. doi:10.1016/j.radphyschem.2024.111701

Lee, H.-J., Kim, S.-W., and Ryu, S.-S. (2015). Sintering behavior of aluminum nitride ceramics with MgO–CaO–Al_2O_3–SiO_2 glass additive. *Int. J. Refract. Met. Hard Mat.* 53, 46–50. doi:10.1016/j.ijrmhm.2015.04.013

Leinweber, G., D.P., S., Trbovich, M. J., Burke, J. A., Drindak, N. J., Knox, H. D., et al. (2006). Neutron capture and total cross-section measurements and resonance parameters of gadolinium. *Nucl. Sci. Eng.* 154, 261–279. doi:10.13182/NSE05-64

Li, L., Jiang, W., Yang, X., Meng, Y., Hu, P., Huang, C., et al. (2024a). From molecular design to practical applications: strategies for enhancing the optical and thermal performance of polyimide films. *Polymers* 16 (16), 2315. doi:10.3390/polym16162315

Li, X. (2023). Customizing MXenes. *Matter* 6 (8), 2519–2522. doi:10.1016/j.matt.2023.05.033

Li, X., Cui, D., Zou, C., Ren, C., and Chen, J. (2024b). Neutron shielding analysis for a gadolinium doped nickel alloy. *Mat. Today Commun.* 38, 107933. doi:10.1016/j.mtcomm.2023.107933

Li, Y., Luo, H., He, Z., Xiang, R., Jia, W., Li, S., et al. (2021). Structural stability and neutron-shielding capacity of $GdBO_3$-$Al_{18}B_4O_{33}$ composite ceramics: experimental investigation and numerical simulation. *Ceram. Int.* 47 (15), 20935–20947. doi:10.1016/j.ceramint.2021.04.092

Li, Y., Zhao, S., and Wu, Z. (2024c). Uncovering the effects of chemical disorder on the irradiation resistance of high-entropy carbide ceramics. *Acta Mater* 277 (277), 120187. doi:10.1016/j.actamat.2024.120187

Lian, X., Xu, W., Zhang, P., Wang, W., Xie, L., and Chen, X. (2023). Design and mechanical properties of SiC reinforced Gd_2O_3/6061Al neutron shielding composites. *Ceram. Int.* 49 (17), 27707–27715. doi:10.1016/j.ceramint.2023.04.092

Lo, J., Zhang, R., and Santos, R. (2015). Machine-able yttria stabilized zirconia composites for thermal insulation in nuclear reactors. *JOM* 68, 463–468. doi:10.1007/s11837-015-1740-x

Malaki, M., and Varma, R. S. (2023). Wetting of MXenes and beyond. *Nano-Micro Lett.* 15, 116. doi:10.1007/s40820-023-01049-x

Mhareb, M. H. A. (2023). Optical, Structural, Radiation shielding, and Mechanical properties for borosilicate glass and glass ceramics doped with Gd_2O_3. *Ceram. Int.* 49 (22), 36950–36961. doi:10.1016/j.ceramint.2023.09.026

Mhareb, M. H. A., Sayyed, M. I., Alonizan, N., Almessier, M. A., Baig, I., AlOtaibi, R., et al. (2024). Radiation shielding, optical, structural, morphological, and thermal features for tellurite glass ceramics. *Nucl. Eng. Technol.* 56 (11), 4708–4715. doi:10.1016/j.net.2024.06.034

Oh, S., Ahn, J.-H., Jung, R., Kim, H.-J., Chu, Y., Choi, D. H., et al. (2023). Characterization of various stainless steels containing gadolinium as thermal neutron absorbing and shielding materials. *Metals* 14 (1), 16. doi:10.3390/met14010016

Onaizi, A. M., Amran, M., Tang, W., Betoush, N., Alhassan, M., Rashid, R. S. M., et al. (2024). Radiation-shielding concrete: a review of materials, performance, and the impact of radiation on concrete properties. *J. Build. Eng.* 97, 110800. doi:10.1016/j.jobe.2024.110800

Oses, C., Toher, C., and Curtarolo, S. (2020a). High-entropy ceramics. *Nat. Rev. Mat.* 5, 295–309. doi:10.1038/s41578-019-0170-8

Oses, C., Toher, C., and Curtarolo, S. (2020b). High-entropy ceramics. *Nat. Rev. Mat.* 5 (4), 295–309. doi:10.1038/s41578-019-0170-8

Oto, B., Kavaz, E., Durak, H., Aras, A., and Madak, Z. (2019). Effect of addition of molybdenum on photon and fast neutron radiation shielding properties in ceramics. *Ceram. Int.* 44 (17), 23681–23689. doi:10.1016/j.ceramint.2019.08.082

Peng, H., Ren, G., Hampp, N., Wu, A., and Yang, F. (2023). The development of rare-earth combined Fe-based magnetic nanocomposites for use in biological theranostics. *Nanoscale* 15, 10513–10528. doi:10.1039/d3nr01373a

Poltabtim, W., Thumwong, A., Wimolmala, E., Rattanapongs, C., Tokonami, S., Ishikawa, T., et al. (2022). Dual X-ray- and neutron-shielding properties of Gd_2O_3/NR composites with autonomous self-healing capabilities. *Polymers* 14 (21), 4481. doi:10.3390/polym14214481

Qi, Z., Yang, Z., Li, J., Guo, Y., Yang, G., Yu, Y., et al. (2022). The advancement of neutron-shielding materials for the transportation and storage of spent nuclear fuel. *Materials* 15 (9), 3255. doi:10.3390/ma15093255

Qi, Z.-D., Yang, Z., Yang, X.-G., Wang, L.-Y., Chang-Yuan, L. I., and Dai, Y. (2023). Performance study and optimal design of Gd/316 L neutron absorbing material for spent nuclear fuel transportation and storage. *Mat. Today Commun.* 34, 105342. doi:10.1016/j.mtcomm.2023.105342

Rachkov, V. I., Kalyakin, S. G., Kukharchuk, O. F., Orlov, Y. I., and Sorokin, A. P. (2014). From the first nuclear power plant to fourth-generation nuclear power installations [on the 60th anniversary of the World's First nuclear power plant]. *Therm. Eng.* 61, 327–336. doi:10.1134/s0040601514050073

Rashad, M., Hanafy, T. A., and Issa, S. A. M. (2020). Structural, electrical and radiation shielding properties of polyvinyl alcohol doped with different nanoparticles. *J. Mat. Sci. Mat. Electron.* 31, 15192–15197. doi:10.1007/s10854-020-04083-2

Rehm, T. E. (2022). Advanced nuclear energy: the safest and most renewable clean energy. *Curr. Opin. Chem. Eng.* 39, 100878. doi:10.1016/j.coche.2022.100878

Rehm, T. E. (2023). Advanced nuclear energy: the safest and most renewable clean energy. *Curr. Opin. Chem. Eng.* 39, 100878. doi:10.1016/j.coche.2022.100878

Saudi, H. A., Hassaan, M. Y., Tarek, E., and Borham, E. (2020). Development of advanced, transparent radiation shielding glass possessing phosphate and lead ions in the glassy matrix. *J. Opt.* 49 (4), 438–445. doi:10.1007/s12596-020-00652-0

Sayyed, M. I., Kaky, K. M., Şakar, E., Akbaba, U., Taki, M. M., and Agar, O. (2019). Gamma radiation shielding investigations for selected germanate glasses. *J. Non-Cryst. Solids* 512, 33–40. doi:10.1016/j.jnoncrysol.2019.02.014

Schelter, T. C. a.E. J. (2019). Rare earth elements: mendeleev's bane, modern marvels. *Science* 363, 489–493. doi:10.1126/science.aau7628

Shah, A. u.R., Prabhakar, M. N., Wang, H., and Song, J.-I. (2016). The influence of particle size and surface treatment of filler on the properties of oyster shell powder filled polypropylene composites. *Polym. Compos.* 39 (7), 2420–2430. doi:10.1002/pc.24225

Shruti, N., and Gurmeet, K. (2022). A mini review on application of boron neutron capture therapy in cancer treatment. *IOP Conf. Ser. Mater. Sci. Eng.* 1225 (1), 012047. doi:10.1088/1757-899x/1225/1/012047

Silva, D. D. S., Nascimento, A. R. C., Koga, G. Y., Zepon, G., Kiminami, C. S., Botta, W. J., et al. (2023). Alloy design for microstructural-tailored boron-modified ferritic stainless steel to ensure corrosion and wear resistance. *J. Mat. Res. Technol.* 24, 418–429. doi:10.1016/j.jmrt.2023.03.023

Soltan, A. (1938). Interaction of fast neutrons with atomic nuclei. *Nature* 142, 252. doi:10.1038/142252a0

Sun, H., Li, N., Zhu, Y., and Liu, K. (2023). A model for direct effect of graphene on mechanical property of Al matrix composite. *Metals* 13 (8), 1351. doi:10.3390/met13081351

Tan, S., Jiang, P., Liu, J., Yang, X., Lai, Y., Hu, X., et al. (2024). Two-step hydrothermal synthesis of $Gd_2O(CO_3)_2$@Bi-MOF/graphene nanoplatelets for enhancing ^{222}Rn and gamma radiation shielding of polymethyl methacrylate-based composites. *Polym. Compos.*, 1–13. doi:10.1002/pc.29316

Tao Yu, J. W. (2018). Spectral analysis of the effects of γ-irradiation on gadolinium-containing barium phosphate glass. *Spectrosc. Spectr. Analysis* 38 (11), 3607–3610. doi:10.3964/j.issn.1000-0593(2018)11-3607-04

Tiamduangtawan, P., Kamkaew, C., Kuntonwatchara, S., Wimolmala, E., and Saenboonruang, K. (2020a). Comparative mechanical, self-healing, and gamma attenuation properties of PVA hydrogels containing either nano- or micro-sized Bi_2O_3 for use as gamma-shielding materials. *Radiat. Phys. Chem.* 177, 109164. doi:10.1016/j.radphyschem.2020.109164

Tiamduangtawan, P., Wimolmala, E., Meesat, R., and Saenboonruang, K. (2020b). Effects of Sm_2O_3 and Gd_2O_3 in poly (vinyl alcohol) hydrogels for potential use as self-healing thermal neutron shielding materials. *Radiat. Phys. Chem.* 172, 108818. doi:10.1016/j.radphyschem.2020.108818

Toher, C., Oses, C., Esters, M., Hicks, D., Kotsonis, G. N., Rost, C. M., et al. (2022). High-entropy ceramics: propelling applications through disorder. *MRS Bull.* 47, 194–202. doi:10.1557/s43577-022-00281-x

Wang, G., Zhang, J., Shen, S., Zhong, L., Mei, L., and Tang, Z. (2022). 3D printing of gadolinium oxide structure neutron absorber. *Ceram. Int.* 48 (23), 35198–35208. doi:10.1016/j.ceramint.2022.08.118

Wang, J.-A., Wang, H., Jiang, H., and Bevard, B. (2018). High burn-up spent nuclear fuel transport reliability investigation. *Nucl. Eng. Des.* 330, 497–515. doi:10.1016/j.nucengdes.2018.02.007

Wang, K., Ma, L., Yang, C., Bian, Z., Zhang, D., Cui, S., et al. (2023). Recent progress in Gd-containing materials for neutron shielding applications: a review. *Materials* 16 (12), 4305. doi:10.3390/ma16124305

Wang, M., Wang, Z., Li, N., Liao, J., Zhao, S., Wang, J., et al. (2015). Relationship between polymer–filler interfaces in separation layers and gas transport properties of mixed matrix composite membranes. *J. Membr. Sci.* 495, 252–268. doi:10.1016/j.memsci.2015.08.019

Ward, T. Z., Wilkerson, R. P., Musicó, B. L., Foley, A., Brahlek, M., Weber, W. J., et al. (2024). High entropy ceramics for applications in extreme environments. *J. Phys. Mater.* 7, 021001. doi:10.1088/2515-7639/ad2ec5

Wei, W., Hong, Y., Yuan, Y., Li, Y., Cui, K., Zhang, T., et al. (2023). Enhanced wide energy regions gamma ray shielding property for Bi_2O_3-$Gd_2O(CO_3)_2$·H_2O/EP composites with strong electron cloud overlap. *J. Alloys Compd.* 938, 168672. doi:10.1016/j.jallcom.2022.168672

Wu, F.-C., and Yu, S.-C. (1988). The effect of SiO_2 and Al_2O_3 additives on the sintering of MgO-containing zirconia. *Mat. Res. Bull.* 23 (12), 1773–1780. doi:10.1016/0025-5408(88)90188-2

Wu, X., Liu, W., Yang, L., and Zhang, C. (2024). Construction of alumina framework with a sponge template toward highly thermally conductive epoxy composites. *Polym. Eng. Sci.* 64 (4), 1812–1821. doi:10.1002/pen.26661

Xu, H., Liu, D., Sun, W.-Q., Wu, R.-J., Liao, W., Li, X.-L., et al. (2022). Study on the design, preparation, and performance evaluation of heat-resistant interlayer-polyimide-resin-based neutron-shielding materials. *Materials* 15 (9), 2978. doi:10.3390/ma15092978

Xu, Z. G., Jiang, L. T., Zhang, Q., Qiao, J., Gong, D., and Wu, G. H. (2016a). The design of a novel neutron shielding B_4C/Al composite containing Gd. *Mat. Des.* 111, 375–381. doi:10.1016/j.matdes.2016.07.140

Xu, Z. G., Jiang, L. T., Zhang, Q., Qiao, J., Gong, D., and Wu, G. H. (2016b). The design of a novel neutron shielding B_4C/Al composite containing Gd. *Mat. Des.* 111, 375–381. doi:10.1016/j.matdes.2016.07.140

Yang, X., Song, L., Chang, B., Yang, Q., Mao, X., and Huang, Q. (2020). Development of Gd-Si-O dispersed 316L stainless steel for improving neutron shielding performance. *Nucl. Mat. Energy* 23, 100739. doi:10.1016/j.nme.2020.100739

Yorulmaz, N., Yasar, M. M., Acikgoz, A., Kavun, Y., Demircan, G., Kamislioglu, M., et al. (2024). Influence of Gd_2O_3 on structural, optical, radiation shielding, and mechanical properties of borate glasses. *Opt. Mat.* 149, 115032. doi:10.1016/j.optmat.2024.115032

Yousefi, T., Torab-Mostaedi, M., Ghasemi, M., and Ghadirifar, A. (2015). Synthesis of Gd_2O_3 nanoparticles: using bulk Gd_2O_3 powders as precursor. *Rare Met.* 34, 540–545. doi:10.1007/s12598-015-0447-z

Yu, Y., Tang, S., and Hu, J. (2016). Effects of heat-treatment on the interfacial reaction and tensile properties of Al_2O_3 coated-$Al_{18}B_4O_{33}$ w/Al–Mg matrix composites. *Mat. Des.* 90, 416–423. doi:10.1016/j.matdes.2015.11.011

Zeng, Y., Chen, X., Sun, L., Yao, H., and Chen, J. (2022). Effect of different sintering additives type on Vat photopolymerization 3D printing of Al_2O_3 ceramics. *J. Manuf. Process.* 83, 414–426. doi:10.1016/j.jmapro.2022.09.022

Zhang, G., Guo, L. a., Cao, R., Zhang, J., and Chen, J. (2008). Cross-section measurement for the 10B(n, α)7Li reaction at 4.0 and 5.0MeV. *Appl. Radiat. Isot.* 66 (10), 1427–1430. doi:10.1016/j.apradiso.2007.07.035

Zhang, P., Jia, C., Li, J., and Wang, W. (2020a). Shielding composites for neutron and gamma-radiation with Gd_2O_3@W core-shell structured particles. *Mat. Lett.* 276, 128082. doi:10.1016/j.matlet.2020.128082

Zhang, Q., Xue, T., Lu, Y., Ma, L., Yu, D., Liu, T., et al. (2023). Fluorine-containing polyimide nanofiber membranes for durable and anti-aging daytime radiative cooling. *J. Met. Sci. Technol.* 179, 166–173. doi:10.1016/j.jmst.2023.07.011

Zhang, Q.-P., Xu, Y.-C., Li, J.-L., Liu, A.-J., Xu, D.-G., Wei, M., et al. (2020b). Hunting for advanced low-energy gamma-rays shielding materials based on $PbWO_4$ through crystal defect engineering. *J. Alloys Compd.* 822, 153737. doi:10.1016/j.jallcom.2020.153737

Zhang, S. (2021). High temperature ceramic materials. *Materials* 14 (8), 2031. doi:10.3390/ma14082031

Zhang, X., Li, Y., Li, C., Yang, F., Jiang, Z., Xue, L., et al. (2021). A novel $(La_{0.2}Ce_{0.2}Gd_{0.2}Er_{0.2}Tm_{0.2})_2(WO_4)_3$ high-entropy ceramic material for thermal neutron and gamma-ray shielding. *Mat. Des.* 205, 109722. doi:10.1016/j.matdes.2021.109722

Zhang, Y., and Bai, X.-M. (2019). Ceramic materials for nuclear energy applications. *JOM* 71, 4806–4807. doi:10.1007/s11837-019-03854-5

Zhong, J., Zheng, X., He, G., Xia, J., and Pu, Z. (2020). Ultralow dielectric constant and high temperature resistance composites based on self-crosslinking polysulfone and hollow glass beads. *J. Electron. Mat.* 49, 7581–7588. doi:10.1007/s11664-020-08491-2

Zhu, X., Zhang, X., and Guo, S. (2022). Constructing oriented two-dimensional fish scale-like Gd@MXene barrier walls in polyvinyl alcohol to achieve excellent neutron shielding properties. *Nanoscale* 14 (29), 10581–10593. doi:10.1039/d2nr02385g